A possible sequence of events for the generalized Glacial-Interglacial cycle

Synte Peacock [1], Emily Lane [2], and Juan M. Restrepo[3]

[1] *Department of the Geophysical Sciences*

University of Chicago, Chicago, IL 60637, U.S.A.

[2] *Department of Atmospheric Sciences*

University of California Los Angeles, Los Angeles, CA 90955, U.S.A.

[3] *Department of Mathematics and Department of Physics*

University of Arizona, Tucson, AZ 85721, U.S.A.

Abstract

There is not yet widespread agreement as to the underlying cause of the 80-100 ppmv roughly 100kyr-duration Glacial-Interglacial cycles in atmospheric pCO_2. Most of the mechanisms which have been proposed to account for the observed variations in atmospheric pCO_2 appear to in some way violate interpretations of paleo proxy data. The inability of a single mechanism to explain the observed cycles in atmospheric CO_2, (which show amazing similarity over the past 430,000 years) is perplexing, and leads us to consider whether a *combination of mechanisms* might be consistent with available evidence.

Consistent with previous work, we find that physical changes (ocean circulation, temperature, mixing) can only explain part of the observed atmospheric pCO_2 variation; changes in ocean chemistry are invoked to explain the remainder. In order to account for the initial pCO_2 drawdown (from Interglacial to intermediate levels), we invoke physical changes in the ocean (mixing, tempearture). The transition from intermediate atmospheric pCO_2 levels to full Glacial conditions involves a small increase in mean-ocean nutrient levels and mean-ocean alkalinity, accomplished by falling sea-level and subsequent erosion of organic-rich shelf sediments. The first part of the transition out of full Glacial conditions is achieved through an increased temperature and increased mixing in the Southern Ocean. The final part of the atmospheric pCO_2 rise up to full interglacial conditions is attained through rising sea-level and the subsequent change in mean-ocean alkalinity and phosphate, and a rise in the northern hemisphere temperature and ocean mixing.

The proposed sequence of events is consistent with most existing

evidence on paleo-nutrient levels and changes in export production over a Glacial-Interglacial cycle. Furthermore, it is consistent with evidence for a whole-ocean shift in δ^{13}C towards significantly more negative values in the Late Glacial. The proposed scenario is also consistent with ice-core-based timing constraints, as summarized by Broecker and Henderson (1998). We show that we are able to explain the full magnitude of the Glacial-Interglacial cycle in atmospheric pCO_2 *without* the need to invoke iron-fertilization in the Southern Ocean.

1 Introduction

Over the last half million years or so, Earth's climate has cycled through a series of fairly regularly spaced Glacial and Interglacial eras. During this time, changes in atmospheric partial pressure of CO_2 (pCO_2) have been strongly correlated with fluctuations in global temperature and ice volume (Petit et al., 1999). During the Last Glacial Maximum (LGM), the pCO_2 of the atmosphere was around 200ppmv, compared with 280ppmv in the preindustrial era. In addition to this 80ppmv drop, the terrestrial biosphere is thought to have added some 500 Pg of carbon to the atmosphere-ocean system during the last Glacial, estimated to be equivalent to an effective 15ppmv increase in atmospheric pCO_2 after $CaCO_3$ compensation (Sigman and Boyle, 2000). While it is generally agreed that the ocean must somehow regulate Glacial-Interglacial changes in pCO_2 on timescales of tens of thousands of years (Broecker and Peng, 1982), the means by which such a coupling might be achieved is still under debate (Sigman and Boyle, 2000).

The typical "Glacial-Interglacial" cycle over the past 430,000 years is characterized by a slow decline in temperature and CO_2 (lasting tens of thousands of years) under low background levels of dust deposition, followed by a period during which dust flux rises, while temperature and CO_2 fall still further, culminating in maximum glacial conditions. The end of the LGM is marked by a rapid decline in dust levels and relatively rapid rise of temperature and CO_2 (taking place over <10,000 years) to full Interglacial conditions. Interglacial periods are far shorter than the corresponding Glacials; then the cycle repeats itself. Prior to 430,000 years ago this 100,000 year cyclicity between Glacial and Interglacial periods was somewhat more muted, but still clearly discernible back to about 740,000 years ago (Augustin et al., 2004).

Although a large number of mechanisms have been proposed to account for the Glacial-Interglacial pCO_2 variations, the combination of data-based constraints and timing constraints make it highly unlikely that any single process can account for the entire change. We here use a box model to explore whether the observed pCO_2 cyclicity can be accounted for by a sequence of distinct processes, both physical and chemical. The proposed sequence of events is tested against both paleo-proxy data from deep-ocean sediment cores and timing constraints from ice-cores. We demonstrate that relatively small physical changes (mixing, rate of circulation, temperature boundary conditions) which are consistent with proxy evidence can only account for part (roughly 50ppmv) of the observed Glacial-Interglacial pCO_2 shift. Examination of the relative timing of CO_2 rise and atmospheric $\delta^{18}O$ suggests that, in the transition from peak Glacial to Interglacial conditions, the last part of the pCO_2 rise is coincident with changing sea-level. We therefore explore the possibility that changes in ocean chemistry triggered by sea-level

Table 1: *Definition of time periods used in this study*

This Study	Age (years)	Marine Isotope Stages
"Interglacial"	0-10	1
"Glacial"	10-75	2, 3, 4
"Intermediate"	75-110	5a-d

change could account for the remainder of the pCO_2 change. The proposed sequence of events is shown to be largely consistent with paleo-nutrient reconstructions, with recent estimates of export production, and with the timing constraints imposed by ice-core records.

In this study, we view the generalized Glacial-Interglacial cycle as consisting of three quite distinct periods. These we term "Interglacial", "Intermediate", and "Glacial" (see Figure 1). The "Intermediate" stage corresponds to Marine Isotope Stages 5a through 5d (roughly 110kyr to 75kyr BP; see Table 1); while "Glacial" corresponds to the time period shaded in light grey in Figure 1 and Figure 3 (roughly 75kyr through 10kyr BP). "Interglacial" periods are those such as the Holocene, where atmospheric pCO_2 levels are close to 280ppmv for a relatively short period of time. The Intermediate stage is characterized by low background dust flux and relatively high (but decreasing) atmospheric pCO_2 (generally higher than 220ppmv). The Glacial period is characterized by high dust fluxes and low atmospheric pCO_2 (generally lower than 220ppmv).

2 Constraints from data

2.1 Proxy-data from the Glacial ocean

During the LGM, the sea surface temperature (SST) was lower than at the present day. Although the CLIMAP project (CLIMAP, 2001) reported a minimal change in the low latitude SST, more recent estimates (Beck et al., 1992; Guilderson et al., 1994) suggest the temperature dropped by between 4°C and 5°C. The evidence for change in the height of the snow-line near the equator also supports a sea surface temperature change of order 5°C (Broecker, 1995). The drop in SST in high latitudes is limited by the freezing

point of seawater. There is now substantial evidence indicating that the southern high latitude regions were around $1-2$°C lower than at the present day, and the northern high latitudes around 3-4°C lower (Broecker, 1995) during the LGM. Martin et al. (2002) calculate that the temperature of the Glacial bottom waters of the ocean were around 2-3°C cooler than the Interglacial. The deep tropical Glacial ocean may have been up to 4°C cooler than during the Interglacial period.

Eustatic sea level changes between the LGM and present day yield an estimate of mean-ocean salinity of between 35.85°/$_{\circ\circ}$ (Fairbanks, 1989) and 35.95°/$_{\circ\circ}$ (Lambeck and Chappell, 2001; Rohling et al., 1998; Yokoyama et al., 2000). Recent data from ocean-floor pore-water profiles (Adkins et al., 2002) imply that the LGM salinity was somewhat higher than this. It has been suggested that ground water reserves or floating ice shelves may explain the discrepancy. Based on this we assume in this study that a mean-ocean salinity of 36°/$_{\circ\circ}$ is representative of the Glacial ocean.

There is evidence for increased sea-ice coverage in the Southern Ocean and a northward migration of the polar front in Glacial times (e.g. Francois et al. (1997)). These authors suggest that increased stratification in the Southern Ocean could be an important factor in lowering atmospheric pCO_2. In a similar vein, Toggweiler (1999) has also proposed increased stratification (reduced mixing) and reduced ventilation of deep water as a mechanism for lowering atmospheric pCO_2.

There are various lines of evidence suggesting that the thermohaline flow in the North Atlantic was weaker during the last Glacial. There is evidence from δ^{13}C and Cd/Ca (Bacastow, 1987; Boyle and Keigwin, 1982; Boyle, 1992) that NADW was found at a considerably shallower depth during the last Glacial than at the present day. Radiocarbon age differences between co-existing planktonic and benthic foraminifera suggest that deep water in the Southern Ocean and Pacific was considerably older during the LGM, perhaps implying a reduced rate of flow (Goldstein et al., 2001; Shackleton et al., 1988; Sikes et al., 2000). Measurements of the authigenic uranium in sediments have been used as a proxy for the amount of oxygen in deep water. This evidence implies that oxygen in the deep ocean was decreased during the Glacial, but that the deep ocean was not anoxic (Francois et al., 1997). However, there is currently some debate as to the interpretation of paleo-circulation proxies. Wunsch (2003) argues that a reduced circulation is hard to reconcile with evidence for stronger winds in Glacial times. There is also evidence from ^{231}Pa/^{230}Th that contradicts the concept of reduced-flow during the Glacial (e.g. Yu et al. (1996)). More recently it has been shown that much of the observed variability in down-core δ^{13}C records can be explained under a steady-state circulation and changing boundary conditions (Rutberg and Peacock, 2005). Until a consensus is reached on the interpreta-

tion of existing circulation proxy-records, it is impossible to say definitively how much Glacial large-scale ocean circulation differed from that of today.

Iron fertilization has been suggested as a mechanism by which to lower atmospheric CO_2 during Glacial periods (Martin, 1990). It has been shown that the addition of a limiting nutrient such as iron can have a very strong local effect on export production in high-nutrient, low chlorophyll (HNLC) regions such as the Southern Ocean, which exhibit 'under-realized utilization potential'. Even a small elevation in the input of iron (via dust) to the Southern Ocean might be expected to increase nutrient utilization, export production (and hence atmospheric pCO_2 drawdown).

What about the evidence for past levels of export production? A recent compilation of various data from a large number of cores by Kohfeld et al. (2005) suggests that net export production was the same or lower than at the present day during much of the Intermediate-stage (Marine Isotope Stages (MIS) 5a through 5d). During the LGM, however, it appears from the Kohfeld compilation that outside of the Southern Ocean, export production may have been somewhat higher than today, whereas south of 50°S export production during the LGM appears somewhat lower than present-day levels. The small increase in dust flux observed during the Intermediate period (stages 5a-d; Figure 1) appears *not* to have been associated with an increase in global export production (Kohfeld et al., 2005). However, the much larger increase in dust flux during the Glacial period (Figure 1) *does* correlate with generally higher global export production.

There is an important distinction between net export production and nutrient utilization. If there is no change in circulation, an increase in nutrient utilization and an increase in export production will go hand in hand. However, if the supply of nutrients to the surface is decreased (for example through enhanced stratification, or reduced vertical mixing), the percentage of nutrients utilized could increase while export production remained constant. Evidence for the degree of nutrient utilization in the Glacial Southern Ocean is somewhat contradictory. There are a number of proxies which have been used in attempt to evaluate the degree of nutrient utilization in the Glacial ocean. Nitrate uptake has been assessed from variations in ^{15}N in organic matter through time (an increase in nitrate uptake would lead to an increase in the ^{15}N of organic matter in the surface ocean). Past levels of phosphate in the Glacial surface ocean have been estimated based on Cd/Ca ratios in planktonic foraminifera. Uptake of silica in the surface ocean has been estimated based on the $\delta^{30}Si$ concentration in diatoms (higher surface water silica uptake would lead to and increase in the $\delta^{30}Si$ of diatoms); and surface-water CO_2 in the Glacial ocean has been inferred based on the $\delta^{13}C$ of organic material (a decrease in surface-water CO_2 would be reflected by a relative increase in the $\delta^{13}C$ of organic material).

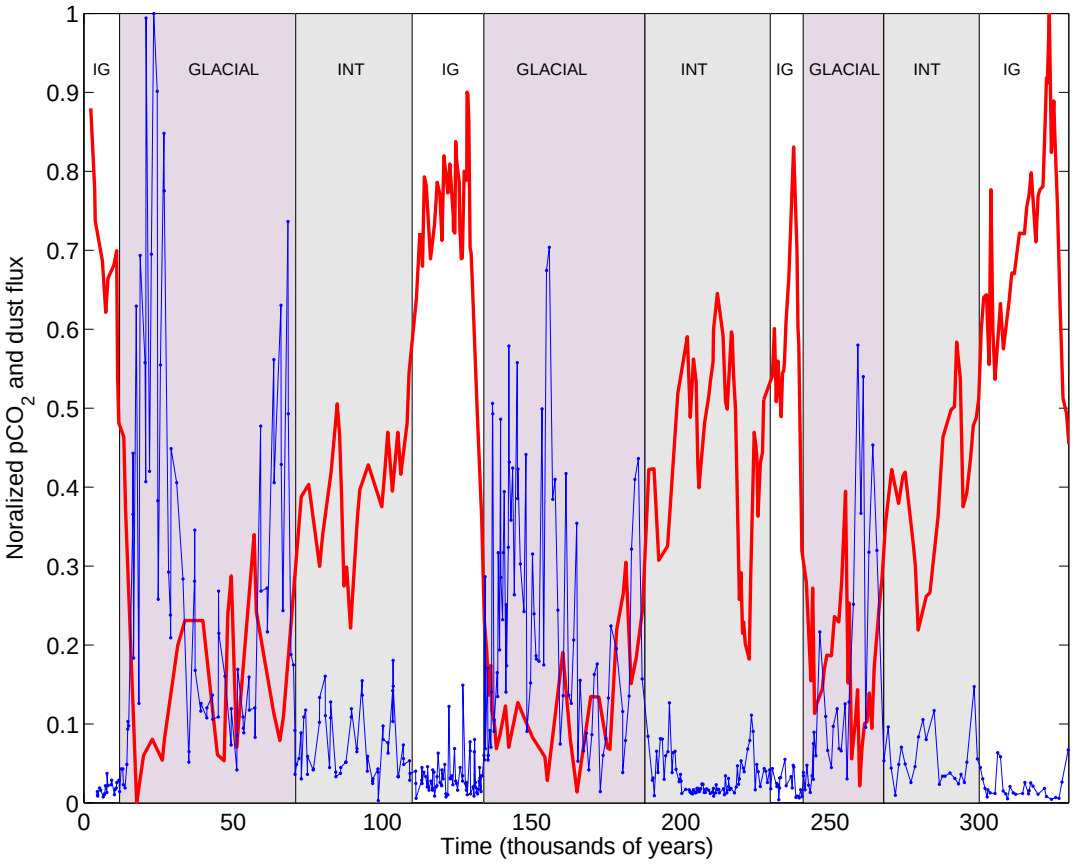

Figure 1: Atmospheric pCO_2 (red) and dust (blue) records from the Vostok ice core. Data are those reported in Petit et al. (1999). Both records have been normalized such that the maximum values over the time period 0-430,000 years scale to +1, and the minimum values to zero (in absolute terms, over the period shown in the figure, the minimum value of pCO_2 is 182 ppmv and the maximum 298ppmv). The shaded regions correspond to time-periods discussed in the text, and during which each model solution was obtained. The Interglacial (IG) periods are those of high (roughly 280ppmv) atmospheric pCO_2 and low background dust flux; 'Intermediate' (INT) periods occur between full Interglacial and full Glacial conditions (grey shading); and for the purposes of this study, 'Glacial' is used to refer to the period with coldest temperatures, lowest atmospheric pCO_2, and highest dust-flux.

Evidence from nitrogen-isotopes suggests that nutrient utilization in the Indian and Pacific sectors of the sub-Antarctic was somewhat greater during the Glacial than in the modern (Interglacial) ocean (Robinson et al., 2005), whereas in the Atlantic sector, nutrient utilization was roughly the same as present-day levels (Robinson et al., 2004). Evidence from Cd/Ca ratios in planktonic foraminifera (Elderfield and Rickaby, 2000; Boyle, 1992) suggests little or no change in nutrient concentrations in the Antarctic surface ocean during the LGM. In fact, if anything, their evidence points to somewhat higher than present-day phosphate levels in the Antarctic, and roughly equivalent to present-day levels in the sub-Antarctic. It appears that the δ^{30}Si in diatoms was lower than at present in the Glacial surface Southern Ocean (DeLaRocha et al., 1998), and surface-water CO_2 appears to have been higher than present-day levels (Rosenthal et al., 2000). Thus the majority of proxy data is consistent with both a decrease in nutrient utilization, *and* a decrease in export production. There are of course uncertainties associated with the Cd/Ca reconstruction; however, error-bounds seem to constrain LGM Antarctic surface-ocean nutrient levels to within 30% of present-day levels. Nitrogen isotopes are the only proxy which suggest increased utilization, and this may be because controls over nitrogen isotope ratios are still not fully understood (Robinson et al., 2005). Based on the available evidence, we feel that increased nutrient drawdown via enhanced iron fertilization in the Glacial ocean is somewhat at odds with the bulk of the evidence for past levels of nutrient utilization.

2.2 Evidence for timing of CO_2 change versus ice-sheet melting

Interesting observations were made by Broecker and Henderson (1998) pertaining to the relative timing of the rise in CO_2 and temperature versus atmospheric δ^{18}O (a proxy for ice sheet melting) coming out of a glaciation. It was observed that, in the transition from the penultimate Glacial to Interglacial, air-temperature and atmospheric pCO_2 in the Southern Hemisphere rose together, some time after the high Glacial dust flux had dropped to low Interglacial levels; the decrease in ice volume and changes in the North Atlantic circulation (as recorded by δ^{13}C in foraminifera) occurred later. The atmospheric CO_2 and temperature (inferred from deuterium) began to rise from low full Glacial values a significant amount of time before the δ^{18}O began to fall (indicating ice sheet melting and change in sea level). Dust had dropped to near-zero levels before the CO_2 rise began. Warming took about 8 thousand years (kyrs). Changes in δ^{13}C in the North Atlantic appear to

occur synchronously with the change in $\delta^{18}O$ (i.e. significantly after the start of the rise in Antarctic temperature and atmospheric pCO_2). The time gap for the last termination is order 2kyr; for the penultimate termination it was order 4kyr (Broecker and Henderson, 1998). Based on the relative timing of events coming out of the penultimate glaciation, Broecker and Henderson (1998) suggest that the trigger for atmospheric pCO_2 change must lie in the tropics or Southern Ocean; not the North Atlantic.

2.3 Criteria which must be satisfied by any model of Glacial-Interglacial atmospheric pCO_2 variations

Taking at face value the Kohfeld et al. (2005) and Elderfield and Rickaby (2000) results, and imposing the Broecker and Henderson (1998) timing constraints, there are certain criteria which should be satisfied by a model of Glacial-Interglacial atmospheric pCO_2 variations:

- Glacial export production in the Southern Ocean should be the same as, or lower than, Interglacial levels
- Glacial export production in the non-polar oceans should be the same as, or higher than, Interglacial levels
- Glacial surface-ocean phosphate concentrations in the Southern Ocean should be the same as, or higher than, Interglacial levels
- Glacial surface-ocean phosphate concentrations in the non-polar oceans should be roughly the same as Interglacial levels
- Export production during the Intermediate stage should be the same as, or lower than, Interglacial levels almost everywhere in the ocean
- Circulation changes in the North Atlantic and ice-sheet melting (sea-level rise) should occur after CO_2 and Antarctic temperatures have already started to rise.
- The compilation of global export production rates combined with the Vostok dust record suggests that, if dust plays any role at all, it most likely does so in the Glacial period.

3 Hypotheses for Glacial-Interglacial pCO_2 Variations

The ultimate cause for the dramatic swings in atmospheric pCO_2 observed on Glacial-Interglacial timescales must lie in the ocean. How exactly such cycles are regulated however, remains elusive. For an excellent review paper on the subject, the reader is referred to Sigman and Boyle (2000). The main ocean-based mechanisms by which the atmosphere's pCO_2 can be altered on millenial timescales are the "solubility pump", the "soft-tissue pump" and the "carbonate pump". These refer to the oceans ability to sequester excess CO_2 due to temperature-induced solubility; change in net amount or utilization of organic matter; and change in the $CaCO_3/C_{org}$ rain ratio and/or dissolution rate of $CaCO_3$, respectively. Another possible way to regulate atmospheric pCO_2 is through changes in physical properties, such as sea-ice cover, mixing, or the ocean's velocity field (Bacastow, 1996; Heinze et al., 1991). While the possible role of locally reduced air-sea gas exchange and/or increased sea-ice cover is still debated (Stephens and Keeling, 2000; Ridgwell, 2001; Archer et al., 2003), there appears to be general agreement that changes in circulation alone will have only a small effect on atmospheric pCO_2 change (Schultz and Paul, 2004; Winguth et al., 1999).

Temperature-Salinity changes: One parameter which is fairly well constrained is the change in mean temperature and salinity of the ocean. During Glacial times, ocean temperatures were lower and mean salinity higher (due to lower ocean volume). Decreasing temperature increases solubility, and hence increases the amount of dissolved CO_2 in the surface ocean; increasing salinity acts in the opposite direction. Results from many studies show that the combined temperature/salinity effect between peak Glacial and Interglacial times was order 20-30ppmv (Sigman and Boyle, 2000); clearly not anywhere near large enough to explain the observed changes.

Shelf Hypothesis: One of the earliest hypotheses put forward to try and account for the observed Glacial-Interglacial atmospheric pCO_2 changes was the so-called "shelf hypothesis" of Broecker (1982). This involves a change in whole-ocean nutrient inventory through phosphorus deposition onto and erosion off shallow shelves which are alternately buried and exposed as sea level rises and falls. Sea level changes are the driving force behind this mechanism. Burial of phosphorus in Interglacials would decrease mean phosphate; erosion in the low-sea level stand of the Glacials would increase mean ocean phosphate. The impact on atmospheric pCO_2 is through changing the mean ocean $\Sigma CO_2 : PO_4$ ratio, which would regulate the extent of pCO_2 drawdown by plants in the surface ocean. This hypothesis has been widely discredited for two reasons: first, it is closely tied to changing sea-level, and second,

because the amount of sediment required to be deposited and eroded on the Glacial-Interglacial timescale in order for this mechanism to account for most of the atmospheric pCO_2 change appears to be far greater than observational evidence suggests.

Alkalinity-change and carbonate-pump-based hypotheses: Because the pCO_2 of surface water in the ocean is a function of both dissolved inorganic carbon (DIC, or ΣCO_2) and alkalinity, changes in the mean ocean inventory of either would have an impact on atmospheric pCO_2 levels. A number of the early hypotheses seeking to explain the Glacial-Interglacial atmospheric pCO_2 variations invoked a change in mean ocean alkalinity (Berger, 1982; Opdyke and Walker, 1992; Milliman, 1993), but again, these hypotheses have been widely discarded because they must be linked to changes in sea level, which occurred during the lattermost part of atmospheric pCO_2 rise.

Hypotheses involving a change in the ocean's carbonate pump seem unlikely because such a change would cause a significant shift in the depth of the lysocline (a transition zone which separates deep-sea sediments with no preserved calcite from shallower sediments where calcite is preserved), which has not been observed. Archer and Maier-Reimer (1994) suggested a way around this problem with a hypothesis which invoked a higher rain rate of organic matter to the seafloor during Glacial times. However, this idea calls for a separation between the saturation horizon and the lysocline, a scenario which Sigman et al. (1998) make a strong case against.

Changes in North Atlantic Circulation: The jury is still out with regard to how to definitively interpret existing evidence for changes in North Atlantic circulation associated with the transition from Glacial to Interglacial periods. There clearly are changes in proxies such as $\delta^{13}C$, but whether such variability reflects changes in boundary properties or in the time-mean circulation remains open to debate (Rutberg and Peacock, 2005). As we will discuss below, there is strong evidence that changes in the North Atlantic significantly lagged the onset of CO_2 and temperature rise as evident from the Vostok ice-core record.

Polar dominance (increased nutrient utilization): Since the mid-1980s, the idea has reigned that polar regions of the ocean are more important in regulating atmospheric pCO_2 than are the low latitude regions. If correct, this would rule out many of the non-polar based mechanisms from having a significant impact on atmospheric pCO_2. Attempts have been made to quantify the "high latitude sensitivity" of a given model by metrics such as the "HBEI" (Broecker et al. (1999); the 'Harvardton Bear Equilibration index, designed to estimate the relative importance of circulation and air-sea gas exchange) and "abiotic pCO_2" (Archer et al., 2000), but how the real ocean fits into all of this is still the subject of ongoing debate (see Lane et

al., 2005 for further discussion).

Because nutrients are largely under-utilized in the Southern Ocean today, it is possible that a significant increase in nutrient utilization in this region during Glacial times could play an important role in the drawdown of atmospheric pCO_2. Many box model results (e.g. Siegenthaler and Wenk (1984); Sarmiento and Toggweiler (1984); Knox and McElroy (1984)) suggest that increased utilization of the currently very under-utilized Southern Ocean nutrients would account for most of the Glacial-Interglacial CO_2 drawdown; but it seems unlikely that so dramatic a change in Southern Ocean nutrient concentrations occurred (Boyle, 1992; Elderfield and Rickaby, 2000). Aside from the proxy evidence for small or no change in Southern Ocean nutrients is the likelihood that a large increase in high-latitude nutrient utilization would cause anoxia in the deep ocean, which also goes against observational evidence (Francois et al., 1997). Furthermore, there is no clear mechanism for a sudden and large high-latitude nutrient drawdown. Iron fertilization is an obvious candidate (Martin, 1990). However, there are problems with this idea. For example, very high dust-fluxes are only observed in Glacial times (as defined in Figure 1), and second, as Broecker and Henderson (1998) point out, the dust flux had fallen to almost zero before the temperature and CO_2 began to rise in the Southern Hemisphere. As a way around this problem, Broecker and Henderson suggest an increase in the rate of nitrogen fixation in the ocean; the idea is that because of the long residence time of nitrate in the ocean, an iron-induced increase in fixed nitrate could take several thousand years to diminish to Interglacial levels.

Increased Sea-ice coverage: Stephens and Keeling (2000) recently proposed that covering most of the Southern Ocean with sea-ice, and hence dramatically reducing air-sea gas exchange, could go a long way towards accounting for the Glacial-Interglacial atmospheric pCO_2 signal by isolating the deep ocean from the atmosphere, and hence increasing the deep ocean storage of ΣCO_2. However, a GCM-based study of the impact of increased sea-ice on atmospheric pCO_2 levels (Archer et al., 2003) suggests that the effect is minimal. There are also box-model based results (Ridgwell, 2001; Lane et al., 2005) which imply that the reduction in air-sea gas exchange that comes from increasing sea-ice cover only has a small net effect on atmospheric pCO_2. Francois et al. (1997) and Toggweiler (1999) suggest that it is more likely that reduced vertical mixing in the Southern Ocean in Glacial times could be an important factor. Gildor and Tziperman (2001) propose a mechanism whereby changes in the North Atlantic are able to remotely trigger a change in extent of Antarctic sea-ice (via deep-ocean circulation); however, their hypothesis relies upon the trigger lying in the North Atlantic, which contradicts timing constraints.

Silicate leakage hypothesis: Brzezinski et al. (2002) suggested an al-

ternative mechanism by which the export ratio of $CaCO_3$ to organic matter might be altered, involving the silicate cycle. Today there is a very strong gradient in silicate in the Antarctic, with high values to the south and low values to the north of the polar front. It is predominantly high-nitrate, low-silicate waters that are exported northward to lower latitudes as Subantarctic Mode Water. The possibility exists that an increase in dust deposition to the Southern Ocean might relieve diatoms from their iron stress, which would feed back to export significantly higher amounts of $Si(OH)_4$ to lower latitudes. This would enhance growth of diatoms over coccoliths, which would lead to a reduction in the export of $CaCO_3$ from the surface ocean, which could subsequently draw down atmospheric pCO_2. Support for this idea is given by the observation that there were higher opal accumulation rates south of the polar front during the LGM (Kumar et al., 1995; Francois et al., 1997), δ^{30}Si measurements indicating a depletion of surface silicic acid during the LGM (DeLaRocha et al., 1998), and δ^{15}N measurements which indicate higher nitrate utilization during the LGM (Francois et al., 1997). It was found in a box-model framework (Matsumoto et al., 2002) that the net effect of such a process could be order 30-40ppmv. However, it must be noted that all the sedimentary evidence, and the large increase in dust flux, occurs in the stage we denote as "Glacial" (Brzezinski et al. (2002), figure 2 therein). By the start of the Glacial (roughly 75,000 years ago for the last Glacial-Interglacial cycle), atmospheric pCO_2 had already dropped from the Interglacial value of around 280ppmv down to around 220ppmv (see Figure 3). Therefore, it seems that the silicate leakage hypothesis could only be invoked to explain the lattermost part of the Glacial decline in atmospheric pCO_2, and not the bulk of the record.

4 Box Model

In order to test our proposed sequence of events, we have constructed a dynamic-flow box model which incorporates a Michaelis-Menten-type feedback on nutrient levels. The model equations can be found in the supplementary material, and details of model construction can be found in Lane et al. (2005). The model geometry is shown in Figure 2. The parameters of the six box model were tuned to achieve the observed pre-industrial pCO_2 of roughly 280ppmv (Barnola et al., 1992) while aiming to stay as close to observational constraints as possible. Initial conditions for each tracer were obtained from estimates of the ocean mean preindustrial tracer values.

Figure 2 shows a diagram of the six-box model. There are three surface boxes representing the Southern "S", non-polar or Equatorial "E", and

Northern oceans "N". The three other boxes are a Deep box "D" (which the Northern box flows into), a deep southern or Intermediate box "I", and a lower or Bottom box "B" (which the southern latitudes flow into). The flows $Q1$ and $Q2 + Q3$ can be thought to represent the North Atlantic Deep Water (NADW) and Antarctic Bottom Water (AABW), respectively.

Mixing coefficients were estimated as follows: The eddy-mixing coefficient for vertical mixing in the interior non-polar ocean was required to be between $1\times10^{-5}\mathrm{m}^2\mathrm{s}^{-1}$ and $1\times10^{-4}\mathrm{m}^2\mathrm{s}^{-1}$, in line with observational evidence (Polzin et al., 1997). In the southern box, where intense mixing along steeply inclined isopycnals yields a very large effective vertical mixing coefficient in depth-coordinates, and in the northern box, where deep convection also yields a high effective mixing, an effective vertical eddy-mixing coefficient of between $10^{-3}\mathrm{m}^2\mathrm{s}^{-1}$ and $10^{-2}\mathrm{m}^2\mathrm{s}^{-1}$ was required. The horizontal eddy-mixing coefficient was estimated to be between 2 and $3\times10^{3}\mathrm{m}^2\mathrm{s}^{-1}$, in line with values used in GCMs. The 'best-guess' mixing coefficient was then multiplied by the area between adjacent boxes and divided by a mean length-scale in order to get an estimate of the volume flux of water exchanged by two boxes by mixing: $F_{Sv} \approx (K_v\times$ Area)/distance. The mixing coefficients are model parameters, and we therefore allowed them to be adjusted to within the ranges specified above. The mixing coefficients used, and the corresponding implied fluxes, are given in Table 2.

Air-sea gas exchange velocities were set to match the mean air-sea gas exchange coefficient (piston velocity) estimated by Broecker and Peng (1982) of 3m/day. The fraction of organic matter which dissolved in the deep (D) box, γ, was set at 80%, with the remainder dissolving in the bottom (B) box (see Figure 1). There is no sedimentary reservoir included in our box model, so all particulate matter leaving the surface boxes is remineralized at depth. From (6) it can be seen that λ, which sets the absolute magnitude of the flows, is also a tunable parameter. This was adjusted to give the Northern flow rate (Q_1) to be around 15 Sv in order to reflect the present magnitude of the NADW (Schmitz, 1995). Table 5 gives the flow rates obtained based on these requirements. The parameters used to obtain this solution are given in Tables 3 and 4. The Redfield ratio $\mathrm{r}_{C:P}$ was calculated assuming that 80% of the particulate flux was organic matter and the remainder $CaCO_3$ (see Toggweiler, 1999 for details) and using the Redfield ratios of Anderson and Sarmiento (1994). The Redfield ratio $\mathrm{r}_{C:P}$=162.5, is that of total carbon to phosphorus. This was obtained assuming an organic carbon to phosphorus ratio, $\mathrm{r}_{Corg:P} = 130$, and that the sinking flux consists of 1 mole $CaCO_3$ for every 4 moles of organic carbon.

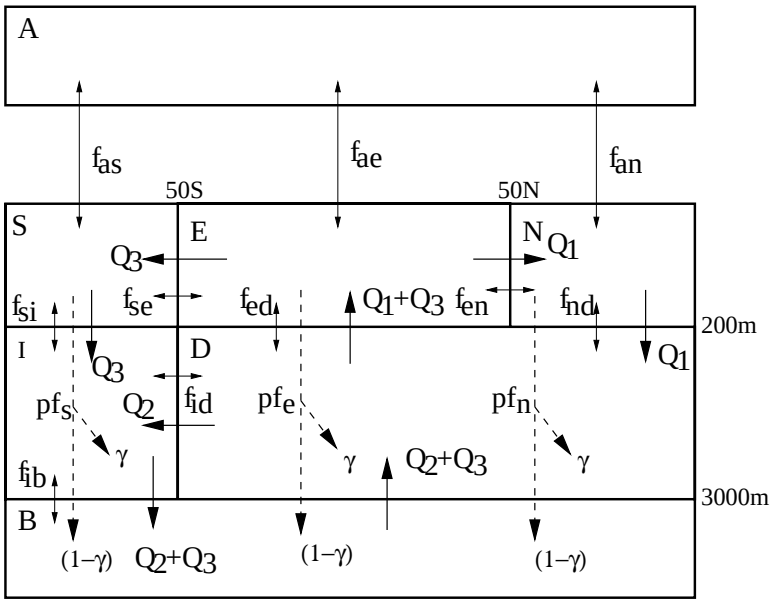

Figure 2: Diagram of the six-box model (not to scale). Shown are the atmosphere (A), the southern surface box (S), the non-polar, or equatorial surface box (E), the northern surface box (N), the deep southern or intermediate box (I), the deep box (D) and the bottom box (B). The density driven thermohaline flow is shown as Q_1, Q_2, and Q_3. f_{xy} denotes mixing between boxes x and y and pf is the particulate flux.

Table 2: *Estimated mixing coefficients, effective fluxes, areas and length-scales from the Interglacial model solution. Area and length scale were prescribed a priori.*

Mixing terms	Eddy-mixing coefficient (m^2/s)	Estimated flux (Sv)	Area (m^2)	Length scale (m)
Vertical				
f_{si}	2.6×10^{-3}	80	4.68×10^{13}	1500
f_{ib}	2.4×10^{-3}	60	4.68×10^{13}	1900
f_{ed}	6.5×10^{-5}	12.5	2.88×10^{14}	1500
f_{db}	6.1×10^{-5}	10	3.13×10^{14}	1900
f_{nd}	2.4×10^{-3}	40	2.52×10^{13}	1500
Horizontal				
f_{se}	2.5×10^{3}	0.3	2×10^{9}	1.7×10^{7}
f_{en}	2.3×10^{3}	0.3	2×10^{9}	1.6×10^{7}
f_{id}	2.5×10^{3}	4	2.8×10^{10}	1.8×10^{7}

Table 3: *Parameter values used in all model solutions*

Parameter		Interglacial and Glacial
Box Volume (10^6 km^3)	Southern	9.36
	Low Latitude	57.6
	Northern	5.04
	Southern Deep	131.04
	Deep	876.96
	Bottom	360
Relaxation time (days)		30
Piston velocity (m/day)		3
Redfield Ratios	r_{CP}	162.5
	r_{OP}	170
	r_{AP}	38
Flow Parameters (km^2/yr)	λ_1	$35,345$
	λ_2	$136,080$
	λ_3	$9,719.7$
	λ_4	$111,340$
	λ_5	$7,952.5$
Freshwater flux (km^2/yr)	Wfs	1.3
	Wfn	0.3

Table 4: *Parameter values used which differed for the Glacial, Intermediate, and Interglacial solutions.*

Parameter		Interglacial	Intermediate	Glacial
Restoring Temperature (°C)	Southern	0	-1.8	-1.8
	Low Latitude	20	16	16
	Northern	5	1	1
Initial Salinity (‰)		34.7	34.7	36.0

Table 5: *Flow rates obtained for thermohaline flow obtained from Interglacial, Intermediate, and Glacial solutions.*

Flow (Sv)	Interglacial	Intermediate	Glacial
Q_1	15.02	11.57	11.57
Q_2	10.61	5.05	5.05
Q_3	8.68	4.13	4.13

Table 6: *Export Flux of Carbon out of each surface box obtained from Interglacial, Intermediate and Glacial solutions.*

Export Flux (g C/m^2/yr)	Interglacial	Intermediate	Glacial
Southern	15.51	15.50	15.53
Non-Polar	29.38	21.91	23.09
Northern	112.35	106.66	108.18
Total (Gt C/yr)	12.02	9.72	10.10

5 A Possible Sequence of Events for the Generalized Glacial-Interglacial Cycle

We have used the box model described in section 4 to test the plausibility of various mechanisms in regulating atmospheric pCO_2, keeping in mind the strong constraints from observational proxy evidence. The model we use improves on previous box models which have been applied to the Glacial-Interglacial pCO_2 problem in that it is not symmetrical (contains distinct high-latitude boxes); it includes a flow-field which is dependent on the model's density field; and includes a Michaelis-Menten type feedback on nutrient levels. More details of model construction and sensitivity to perturbations can be found in Lane et al. (2005). Before using the model to test our proposed sequence of events, we present data from the modern (Interglacial) ocean as a benchmark against which to test the model's Interglacial solution. We then present a series of model solutions, each obtained by making sequential changes to the model which are consistent with existing data. The first step is to investigate the impact on atmospheric pCO_2 of changing only the external (T/S) boundary/initial conditions. We then explore whether the model can yield an "Intermediate" solution (aiming for a pCO_2 of roughly 220ppmv; see Figures 3, 6) and consider whether, to achieve this, we are violating any of the Glacial proxy data. We then investigate what changes must be made to the model in order to achieve the transition from intermediate pCO_2 (c. 220ppmv) to the low pCO_2 (c. 200ppmv) characteristic of full Glacial conditions. Finally, we suggest how the transition from full Glacial back to full Interglacial conditions may have occurred.

5.1 Interglacial data

Using the Levitus ocean data (Conkright et al., 1994), mean and standard deviations for the tracers temperature, salinity and oxygen were calculated for the different regions of our box model (Table 7). These values were used as a benchmark against which to compare the model's Interglacial solution (we are assuming that modern data is representative of the Holocene). Note that there are large standard deviations associated with all these numbers because boxes cover such a large volume of ocean. It is not to be expected that the model match the mean values reported in Table 7 exactly. Rather, the model values should ideally fall within the one standard-deviation errorbars on the data, and should also preserve the relative gradients observed in the tracer data.

Data from Takahashi et al. (1999) was used to calculate the average dif-

Table 7: *Mean and standard deviations (s.d.) for temperature, salinity and oxygen in the regions of the ocean corresponding to the different model boxes. Values were computed from the Levitus annual average dataset, with the Arctic Ocean excluded from the averaging due to spurious values in this region. Values are given for the southern surface box (S), the non-polar, or equatorial surface box (E), the northern surface box (N), the deep southern or intermediate box (I), the deep box (D) and the bottom box (B).*

Tracer		S	E	N	I	D	B
T	mean	1.69	19.03	5.66	1.35	4.39	1.15
(°C)	s.d.	2.55	6.58	3.28	1.20	3.66	0.72
S	mean	34.13	35.17	33.95	34.64	34.70	34.73
(‰)	s.d.	0.23	0.98	1.16	0.14	0.46	0.08
O_2	mean	304.02	202.24	275.24	203.97	145.44	184.66
(μmol/kg)	s.d.	33.76	53.81	47.98	12.89	71.75	36.79

ference in pCO_2 between each surface ocean box and the atmosphere. If the pCO_2 of the surface ocean is less than that of the atmosphere then the ocean will be a sink of pCO_2 and vice versa. In the present-day ocean, the northern high latitudes are by far the most important net sink of CO_2, with $\Delta pCO_{2n} = pCO_{2n} - pCO_{2a} \approx -26$ppmv (see figure 2 for boxes corresponding to subscripts). The mid- and low-latitude regions have a slight excess of pCO_2 with $\Delta pCO_{2e} \approx 3$ppmv. The Southern Ocean is more-or-less neutral. Averaging the Takahashi data reveals that the ocean south of 50°S is only just a net sink of carbon dioxide with $\Delta pCO_{2s} \approx -1$ppmv, but with large enough scatter in the data to make this small offset insignificant. There is also sensitivity to the boundaries selected to define high and low-latitudes. For example, if the cut-off between high and low latitudes is taken to be 40°, rather than 50°, then ΔpCO_{2e} increases to 8ppmv and ΔpCO_{2s} drops to -7ppmv.

Alkalinity in the deep ocean is around 2350μ-eq/kg; in the surface ocean it is around 2280μ-eq/kg; Total CO_2 in the deep ocean averages around 2280μmoles/kg; in the low latitude surface ocean it is roughly 1930μmoles/kg (Toggweiler et al., 2003). The following mean ocean phosphate values were assumed: 1.5-1.6μmol/kg for the southern box; 0.7-0.8μmol/kg for northern box; 0.2μmol/kg for non-polar box.

To estimate global average rates of export production, we use estimates provided by Falkowski et al. (1998), who estimated a total net export production for the present day of order 16 Gt C/yr. The Falkowski study revealed the highest export production in the Northern Hemisphere; elevated levels in eastern mid and low-latitude basins (upwelling-related), with very high concentrations along western continental margins, and near-zero values in the subtropical gyres. The Southern Ocean is characterized by very sharp gradients in export production associated with the frontal systems.

5.2 Interglacial Model State

The restoring ocean-surface temperature boundary condition used to obtain the Interglacial (modern) solution was 0°C for the southern box; 20°C for the non-polar box, and 5°C for the northern box. These values are not the exact average values computed from the Levitus data, but are well within the one standard deviation error-bar. The reason for using values slightly lower than the averages in the high-latitude boxes is that this brings the deep-ocean temperature more into line with observations. In the real ocean, deep convection occurs on a very localized scale in cold high-latitude waters. The mean tracer values of the high-latitude boxes in the box model are somewhat different to the tracer properties which are communicated to the deep ocean

via the process of deep convection. This is a fundamental short-coming of box models in general, and one reason why it is quite difficult to match observed deep-ocean properties in such a framework.

The parameters used in obtaining the Interglacial solution are given in Tables 2 through 6. Table 8 gives the concentrations of tracers predicted by the model for the Interglacial solution. The salinity and oxygen concentrations predicted by the model are, for the most part, within the one-standard deviation error-bar computed from the data. However, in the bottom box, the model oxygen is slightly lower than one standard deviation from the Levitus average, and in the deep box, the oxygen concentration is significantly lower than the mean (although within the one standard-deviation error-bar). This reveals a fundamental limitation of this model; in order to increase the deep and bottom oxygen, either the vertical mixing must be increased, or the high-latitude export production must be reduced. A significant decrease in export production is required to obtain a relatively modest increase in deep-ocean oxygen concentration, while increasing vertical mixing increases the high-latitude nutrient concentrations to values above those observed. Because the model includes a Michaelis-Menten type feedback on surface nutrient concentration (see Lane et al., 2005 for details), increasing the nutrient concentration also increases the particulate flux, which leads to higher oxygen consumption in the deep ocean. One possible resolution to this dilemma is to develop a model with higher vertical resolution. It doesn't seem possible with the current configuration of the model to have a significantly higher deep oxygen concentration and maintain a phosphate concentration in the northern box between 0.7μmol/kg and 0.8μmol/kg, which is in line with observational evidence. The approach taken with earlier box model studies (Sarmiento and Toggweiler, 1984; Knox and McElroy, 1984; Toggweiler, 1999) was to construct a model with just one high latitude box, and to allow the mean phosphate concentration to be very high (much higher than Northern Hemisphere observations, closer to that in the Southern Hemisphere) in this box. This, combined with high vertical mixing, and a very low particulate flux (an order of magnitude lower than Falkowski et al., 1988 estimates) resulted in oxygen levels in the deep boxes somewhat higher than those reported here, but this is clearly at the expense of approximating reality in other areas.

The phosphate concentrations in this solution are in good agreement with observational evidence. The southern box has a value of around 1.5μmol/kg the northern box of just over 0.7μmol/kg; and the non-polar box of 0.15μmol/kg. It should be remembered that the non-polar box extends to 50°N and 50°S. The surface pCO_2 is in fair agreement with the Takahashi et al. (1999) data. The model's northern high latitudes is a sink of CO_2, while the low latitudes and southern box are a source. Also in agreement with present-day observa-

Table 8: *Solution for Interglacial ocean. Temperature is given in* $^\circ C$*, salinity in* $^\circ/_{\circ\circ}$*. The concentrations of* PO_4*,* ΣCO_2 *and* O_2 *are given in* $\mu mol/kg$*,* pCO_2 *is given in ppmv and alkalinity is given in* $\mu eq/kg$*. A, S, E, N, I, D and B correspond to the regions illustrated in Figure 1.*

Tracer	A	S	E	N	I	D	B
T	-	0.1537	19.9543	5.2391	2.0076	4.7121	2.2567
S	-	34.5551	34.9824	34.7942	34.6229	34.7219	34.6320
PO_4	-	1.5337	0.1589	0.7159	2.0294	2.2990	2.4052
ΣCO_2	-	2136.07	1946.52	2053.82	2228.81	2290.39	2291.52
pCO_2	278.20	287.62	280.18	243.97	-	-	-
ALK	-	2292.42	2266.43	2276.04	2315.43	2331.75	2330.27
O_2	-	329.21	232.90	304.76	197.12	81.52	126.80

tions, the northern ocean is much further out of local equilibrium with the atmospheric pCO_2 than either the low latitude or southern box. The northern downwelling is just over 15 Sv. The southern downwelling is around 8 Sv giving a total surface downwelling of 23 Sv.

The export production in the Interglacial solution follows a similar spatial gradient to that of Falkowski et al. (1998), with a total global export production of 12.02 Gt C/yr. It should be noted that this number is significantly higher than the total export production in most carbon box-models, which tend to be about an order of magnitude lower (see Archer et al., 2000, and figure 7 therein for discussion).

5.3 "Interglacial" through "Intermediate" stages

As can be seen from Figure 3, the "Intermediate" stage is characterized for the most part by a low background dust flux, and pCO_2 levels intermediate between the Interglacial and Glacial stages. In order to explain the drop from Interglacial atmospheric pCO_2 levels (c. 280ppmv) to roughly 220ppmv during the Intermediate stage, we wish to call upon mechanisms which are consistent with paleo proxy data. Dust levels are low throughout this period, and the results of the Kohfeld et al. (2005) study suggest export production was for the most part the same as, or lower than, at the present day. Based on these results, we seek a solution which does not invoke any increase in export production to draw down atmospheric pCO_2. Nor do we want to invoke any hypotheses related to changing sea-level at this stage. This is based on results from Lambeck and Chappell (2001) and Siddall et al. (2003), who show that most of the fall in sea-level associated with the Glacial-Interglacial cycle occurred later in time. We are reluctant to change the $CaCO_3/C_{org}$ rain ratio, as this presents difficulties with some of the paleo evidence (see Sigman and Boyle (2000) for discussion), and there seem to be persuasive arguments that the necessary decoupling of lysocline and calcite saturation depth is unlikely.

So what options are left that do not fly in the face of proxy evidence? One obvious mechanism (which has been suggested before - e.g. see Toggweiler (1999); Stephens and Keeling (2000)) is a reduction in the amount of high-latitude mixing as sea-ice begins to spread equatorward with declining temperatures. In the high latitudes there is evidence for advance of sea-ice with encroaching cold (Francois et al., 1997). One effect of increasing sea-ice coverage would be to increase ocean stratification beneath the sea ice (i.e. to reduce vertical mixing).

The model described in Section 4 (and in greater detail in Lane et al., 2005) is used to explore whether or not the Intermediate-stage CO_2 draw-

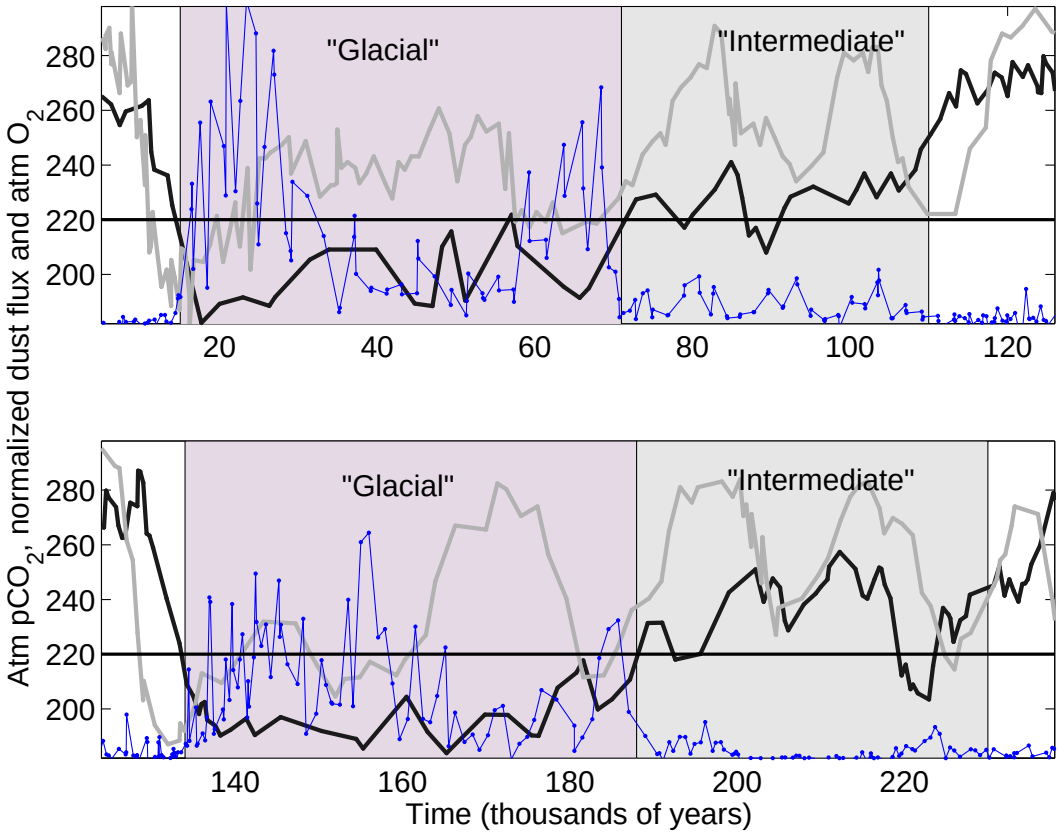

Figure 3: Records of normalized dust (blue), normalized, inverted atmospheric δ^{18}O (grey) and pCO_2 (black) from the Vostok ice core over the last two Glacials. The shading shows the partitioning into "Intermediate" and "Glacial" periods, as defined in the text.

down (roughly 280ppmv to 220ppmv) can be achieved by just changing the temperature restoring boundary condition, and allowing a modest reduction in high-latitude mixing in our model framework. Our imposed Glacial change in restoring temperature represents northern and southern high latitude cooling of 4°C and 1.8°C respectively, and a cooling of the non-polar box by 4°C (Table 4). If the only changes made in the model are to reduce the temperature restoring boundary conditions to Glacial values, the atmospheric pCO_2 drops from 278ppmv to 255ppmv. Many previous studies have noted that the the combined effect of a reduction in temperature boundary condition and an increase in mean salinity can only explain a small fraction of the observed Glacial-Interglacial pCO_2 difference (Sigman and Boyle, 2000); the combined T-S effect has generally been found to be between 20ppmv and 30ppmv. Consistent with this, we find that the net effect of the Glacial combined temperature/salinity boundary conditions would be a 21ppmv reduction of atmospheric pCO_2 in our model. Because decreasing the mean salinity actually increases atmospheric pCO_2, the temperature effect alone is 23ppmv. As discussed earlier, due to the timing constraints on events, we require that the sea-level change (and hence salinity change) occur after the temperature change.

If the only change made to the Interglacial model (after reducing the Glacial temperature restoring boundary condition) is to lower the southern mixing term, f_{si}, by 50% (see Figure 2), the atmospheric pCO_2 drops to 232ppmv. If both vertical mixing terms in the southern box (f_{si} and f_{ib}) are reduced by 50%, the resulting atmospheric pCO_2 is 227ppmv. A 70% reduction in f_{si} from its Interglacial value and no change in other mixing terms results in an atmospheric pCO_2 reduction to 217ppmv; a reduction in both f_{si} and f_{ib} by 70% causes a drawdown to 210ppmv. A measure of the sensitivity of atmospheric pCO_2 to various mixing terms is given in Figure 4, which shows how atmospheric pCO_2 responds when the high latitude mixing terms f_{si}, f_{ib} and f_{nd} are reduced either individually or in combination (the lines are terminated at a point at before which zero-oxygen concentrations are reached in the deep ocean.) Reducing the southern box mixing term f_{si} is slightly more effective at drawing down atmospheric pCO_2 than is reducing the f_{nd} term; this is also evident from the linearized sensitivity analysis discussed in Lane et al. (2005). A reduction of atmospheric pCO_2 to order 220ppmv can be achieved either by reducing both the southern mixing terms to some 40% of their Interglacial levels, or by concurrently reducing all high latitude mixing terms to around 60% of Interglacial levels.

The limitation one runs into when invoking reduced vertical mixing to achieve a draw-down of pCO_2 is that decreasing mixing causes a dramatic decrease in the amount of high-oxygen water supplied to the deep ocean. Approaching anoxic levels, therefore, becomes a problem. As discussed in

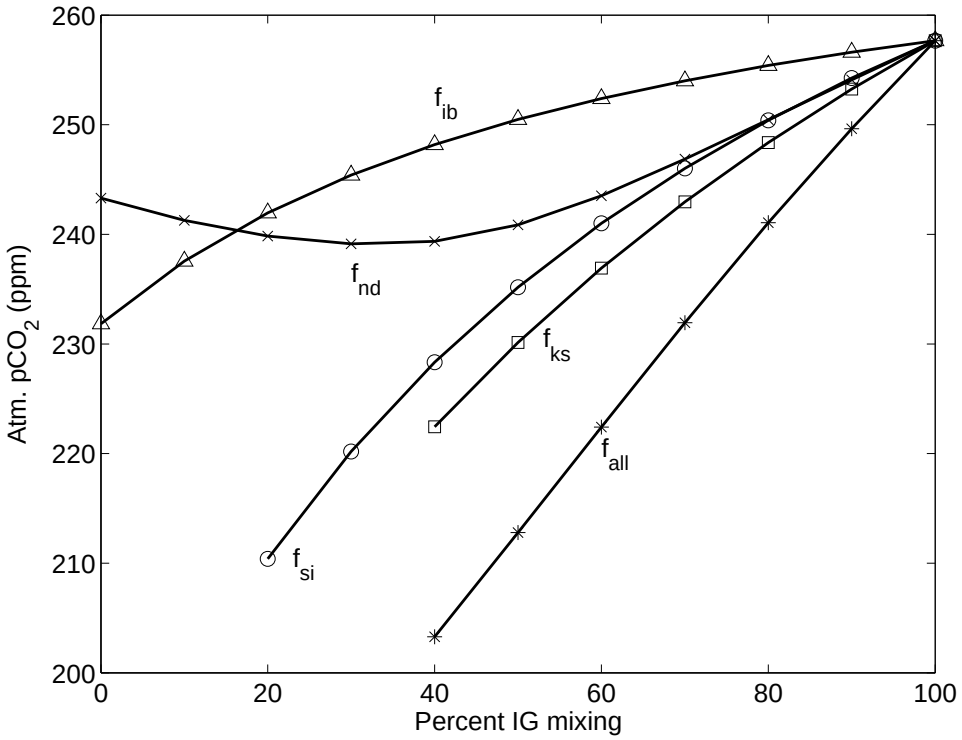

Figure 4: Dependence on atmospheric pCO_2 on various mixing terms in the box model. The starting point is 257ppmv, achieved by imposing 'Glacial' temperature boundary conditions and salinity initial condition (see Table 3) on the model. The triangles represent changes to only the term f_{ib}; crosses represent changes to only the term f_{nd}; open circles to only the term f_{si}; squares to both the southern box mixing terms simultaneously; and stars to all three high-latitude mixing terms simultaneously.

Section 5.2, this model has Interglacial deep and bottom oxygen concentrations which are roughly one standard-deviation below the mean. Because of this there is little room to manoeuver as far as utilizing deep oxygen is concerned. If a solution can be found in which the deep ocean is still oxic, it is likely that the required level of oxygen consumption is entirely within reasonable bounds. In the reduced-mixing solutions mentioned above, the deep ocean oxygen levels are low, but nowhere is the ocean anoxic. Counteracting the decreased deep oxygen through vertical mixing is the particulate flux: lower mixing means less high-nutrient water is brought to the surface; this in turn leads to a reduction in the particulate flux, which will lead to less oxygen being consumed in the deep ocean. However, in the experiments mentioned above, this effect is small relative to the deep oxygen depletion by decreased mixing.

To summarize, in going from the Interglacial (c. 280ppmv) solution to the Intermediate-stage (c. 220ppmv) solution, the following changes were made to the model:
1. the temperature boundary condition was reduced to Glacial values (see Table 4);
2. the northern mixing term was reduced by 30% and the southern mixing terms by 40%.

The results are shown in Table 9. In going from the Interglacial solution (Table 8) to the Intermediate-stage solution (Table 9), there was a global 20% reduction in net export production; nearly all of this reduction is in the non-polar and northern surface boxes (there is very little change in export production in the southern box of the model). Lower net export production during the Intermediate-stage than at the present day is consistent with the findings of Kohfeld et al. (2005). The relatively high nutrients in our model solution in the polar oceans are consistent with the constraints from Cd/Ca and δ^{13}C . The deep oxygen levels are reasonable (especially given the caveat of initially low deep oxygen discussed in section 5.2). The 222ppmv Intermediate-stage model therefore appears to be in fair agreement with much of the existing proxy data.

The next step is to ask what parameter changes are necessary to achieve a transition from intermediate atmospheric pCO_2 levels of 220ppmv to the Glacial values of c.190-200ppmv, and whether the changes required to achieve such a transition are consistent with proxy evidence and timing constraints.

Table 9: *Solution for "Intermediate" stage. Caption as for Table 8.*

Tracer	A	S	E	N	I	D	B
T	-	-1.72	15.97	1.21	0.21	2.15	0.51
S	-	34.44	35.07	34.83	34.58	34.73	34.61
PO_4	-	1.52	0.06	0.39	2.10	2.22	2.60
ΣCO_2	-	2115.2	1939.5	2026.5	2239.1	2287.1	2324.4
pCO_2	222.63	235.84	224.65	180.97	-	-	-
ALK	-	2284.7	2268.3	2266.1	2315.9	2329.3	2336.2
O_2	-	341.0	253.4	327.9	165.6	69.2	69.2

5.4 "Intermediate" through "Glacial" Stages

5.4.1 Meeting proxy-data and timing constraints

During the "Glacial-stage" (marine isotope stages 2,3,4), temperatures continued to fall, ice volume continued to increase, and the dust flux spiked to values significantly above Intermediate-stage and Interglacial levels. As summarized in Section 2.1, proxy evidence suggests that nutrient levels south of the polar front were if anything slightly higher than present-day levels (Elderfield and Rickaby, 2000); while export production in this region appears *not* to have been higher (possibly slightly lower) than today (Kohfeld et al., 2005). Interestingly, the Kohfeld et al. (2005) compilation suggests that export production in the non-polar ocean during the Glacial was actually higher than at the present day. $\delta^{13}C$ records show significant trend toward strongly negative values in the Glacial (Curry et al., 1988; Duplessy et al., 1988). It is of interest to note that many cores exhibit a sharp drop in both benthic and planktonic $\delta^{13}C$ at around 65kyrs BP (e.g. Duplessy et al. (1988), figure 3 therein). This is roughly the time at which we defined the transition from Intermediate-stage to Glacial. The very significant offset in whole-ocean $\delta^{13}C$ between these two time periods lends further support to the notion that there was a fundamental difference in mechanisms regulating the atmospheric pCO_2 content between the Intermediate and Glacial periods.

It would be difficult to significantly increase the export production in the non-polar ocean if nutrient levels were similar to present-day levels (phosphate is already close to zero in most of the non-polar ocean) unless there was a corresponding increase in the supply of nutrients to the surface ocean.

One way this could be accomplished is via increased upwelling. However, our model implies that if anything, the rate of upwelling was somewhat lower, due to a slightly smaller lateral density gradient. Another way to increase nutrient levels would be to increase mean-ocean nutrient inventory. This was one of the early ideas put forward to account for Glacial-Interglacial atmospheric pCO_2 drawdown, but has been widely discredited because the mechanism is crucially tied to sea level, and coming out of glaciations, much of the pCO_2 increase occurred *before* the change in sea-level (ice sheet melting). Furthermore, it is unclear that there is sufficient organic-rich sediment deposited and eroded between Glacial and Interglacial periods to account for the full magnitude of the observed Glacial-Interglacial $\delta^{13}C$ change. Another possibility is that the mean-ocean alkalinity increased during Glacial periods.

Both the whole-ocean nutrient ("shelf") and alkalinity ("coral-reef") hypotheses are intimately tied to changes in sea level. The shelf hypothesis relies on increased deposition of organic-rich material in shelf areas during Interglacial (high sea-level) periods and enhanced erosion of this material during Glacial (low sea-level) periods. Storage and release of phosphorus in marine shelf sediments on Glacial-Interglacial timescales would lead to changes in whole-ocean phosphate inventory. By the beginning of full Glacial conditions (c. 70Kyr for the most recent Glacial-Interglacial cycle), atmospheric $\delta^{18}O$ records suggest that ice sheets were significantly larger, and hence sea level was considerably lower than in Interglacial times. This is supported by sea-level reconstructions (Lambeck and Chappell, 2001; Siddall et al., 2003). A low-stand in sealevel would expose phosphate-rich shelf sediments, the erosion of which could lead to an increase in mean-ocean PO_4. Sea-level changes are required to drive erosion from and deposition onto shallow shelves. If deposition of organic rich sediments occurs on shelves, it would happen during post-glacial sea-level rise.

The coral-reef hypothesis invokes an increase in the magnitude of and shift in the locus of carbonate deposition from the deep sea during Glacials to shelves during Interglacial periods. Existing evidence pertaining to the timing of sea-level changes during the last Glacial suggest that most of the sea-level rise occurred in the latest stages of the Glacial period, with a rise of 100-120m occurring between 20-10kyr BP (Lambeck and Chappell, 2001; Siddall et al., 2003).

5.4.2 Changes in whole-ocean nutrient inventory

In today's ocean there exists a strong correlation between phosphate and $\delta^{13}C$. The reason for this is that variations in $\delta^{13}C$ are due mainly to photosynthesis and respiration; the distribution of phosphate is also mediated by biological activity. Because formation and destruction of temporary organic

carbon reservoirs would be expected to leave a signature in the $^{12}C/^{13}C$ ratio of ocean ΣCO_2 , it might be expected that the Glacial $\delta^{13}C$ distribution could yield information on phosphate levels in the Glacial ocean.

In general, Glacial benthic foraminifera tend to have a lower $^{12}C/^{13}C$ than Interglacial benthic forams. Broecker (1982) made an attempt to compile the deep-ocean $\delta^{13}C$ records existing at the time in order to estimate the mean-ocean $\delta^{13}C$ shift between the LGM and the Holocene, and estimated a net shift of $0.7‰$ towards lower mean-ocean $\delta^{13}C$ in Glacial times. More recently this estimate has been lowered to between $0.32‰$ (Duplessy et al., 1988) and $0.46‰$ (Curry et al., 1988). An increase in mean-ocean $\delta^{13}C$ from Glacial to Interglacial implies removal of carbon from the ocean at the end of the Glacial period to form organic matter, which could be either shelf or terrestrial material. Because deposits of Holocene organic-rich shelf sediments sufficiently large to explain the observed $\delta^{13}C$ shift have not been found, there is general acceptance that most or all of this shift can be attributed to changes in the size of the terrestrial biosphere (Shackleton, 1977; Sigman and Boyle, 2000). Deposition of organic-rich shelf sediments would cause a change in mean-ocean phosphate and $\delta^{13}C$; storage of organic material in the terrestrial biosphere would change mean-ocean $\delta^{13}C$ but would not have any impact on mean-ocean phosphate.

The shelf hypothesis requires that the loss of $\delta^{13}C$ to organic matter in the Interglacial would be compensated by an equivalent loss of ΣCO_2 to $CaCO_3$, such that about a mole of carbon would be removed as $CaCO_3$ for each mole of carbon removed as organic material. In addition to this, roughly one unit of alkalinity would be lost for each unit of ΣCO_2 . The deposition of organic material as shelf sediment would alter the PO_4:ΣCO_2 ratio in the deep ocean. This would lead directly to a larger reduction in pCO_2 due to plant growth in the surface ocean through an increase in export production.

Assuming a mean ocean $\delta^{13}C$ change between peak Glacial and Interglacial times of $0.7‰$, Broecker (1982) estimated that mean deep-ocean PO_4 rose from an Interglacial value of around 2.25μmol/kg to a Glacial value of about 3.2μmol/kg. This estimate should be revised in light of more recent estimates ofthe whole-ocean change in $\delta^{13}C$ (current estimates range from 0.32-$0.46‰$; Curry et al. (1988); Duplessy et al. (1988); Broecker and Henderson (1998)). Following the methodology adopted by Broecker (1982), it is possible to put upper and lower bounds on the mean phosphate concentration in the Glacial ocean (see supplementary material for details). If we assume that the entire Glacial-Interglacial $\delta^{13}C$ shift can be attributed to the deposition of organic-rich sediments, the mean deep-ocean phosphate during Glacial conditions must have been roughly 2.85μmol/kg. If on the other hand it is assumed that the entire $\delta^{13}C$ shift in benthic forams between Glacial and Interglacial times can be attributed to a change in the size of the terrestrial

biosphere, the mean deep-ocean phosphate during Glacial times must have been roughly 2.3μmol/kg. Assuming that a third of the observed δ^{13}C shift can be attributed to the storage and erosion of organic-rich sediments yields an estimate of 2.42μmol/kg for the mean-ocean phosphate.

Even if the observed benthic δ^{13}C change can be attributed wholly to changes in the terrestrial biosphere, the mean-ocean phosphate concentration must have been slightly higher than today during the peak of the last Glacial (the volumetric effect). It is to be expected that an increase in mean-ocean phosphate will act to draw down atmospheric pCO_2 through increased nutrient utilization in the low-latitude ocean (where phosphate concentrations are currently close to zero). We have explored the effect of various assumptions about the degree to which Glacial mean-ocean phosphate was increased over present-day values in our model. If the mean phosphate concentration in the box model is increased so as to roughly achieve the mean deep-ocean phosphate value of 2.85μmol/kg, atmospheric pCO_2 drops from 222ppmv to 182ppmv. In order to achieve a mean deep-ocean phosphate value of 2.42μmol/kg, atmospheric pCO_2 drops from 222ppmv to 209ppmv. If only the volume-based phosphate change of 2.30μmol/kg is used, atmospheric pCO_2 drops from 222ppmv to around 216ppmv.

It is important to note that the model we use does not allow for carbonate compensation, or any kind of feedback between $CaCO_3$ and atmospheric pCO_2. Therefore, while recognizing that removal of carbon in the form of shelf and/or terrestrial organic matter in Glacial periods would entail change in the average ΣCO_2 and alkalinity of the ocean, this is not a process we are able to accurately simulate in the current model. In exploring the effect of increased phosphate, we did not make corresponding increases in ΣCO_2 and alkalinity. Had we included these changes, the net effect would be to lower atmospheric pCO_2 still further.

The volume-based phosphate increase has only a very minor effect (order 6ppmv) on atmospheric pCO_2 . If the entire benthic δ^{13}C change can be attributed to storage/erosion in organic-rich shelf sediments, the estimated change in mean-ocean phosphate is large enough to account for a significant drawdown in atmospheric pCO_2 (order 40ppmv). However, this appears to be at odds with the sedimentary record. (This magnitude of change would require the deposition of 1-2m of sediment containing roughly 1% by weight carbon over the entire ocean shelf area (Broecker, 1982)). A shift in benthic δ^{13}C of -0.46$^\circ/_{\circ\circ}$ requires that roughly 6×10^{16} moles of carbon must have been converted to organic carbon at the end of the Glacial. If only a third (i.e. 0.15$^\circ/_{\circ\circ}$) of the benthic δ^{13}C is attributed to storage in shelf sediments, this requires the burial of roughly 2×10^{16} moles carbon. Assuming organic-rich shelf sediment contains 1% wt carbon, this is equivalent to roughly a 1m-thick layer of sediment spread over the entire ocean shelf area ($\approx3\times10^{17}$cm^2), or

equivalently, a 10m-thick layer of sediment spread over a tenth the ocean shelf area ($\approx 3\times10^{16}$cm^2). On the largest of the world's shallow shelves, the Sunda Shelf, (area roughly 1.8×10^{16}cm^2, Hanebuth et al. (2000)), sediment cover is only a few centimeters, but Holocene sediments over 10m thick have been observed, for example on the central Vietnamese Shelf (Schimanski and Stattegger, 2001). Both the question of timescales of carbon removal/deposition, and the question of whether or not sufficient Holocene-age organic-rich sediment exists to account for burial and erosion of some 2×10^{16} moles carbon on a Glacial-Interglacial timescale, remain questions for future research.

5.4.3 Changes in whole-ocean alkalinity

Among the earliest explanations to be put forward to explain the Glacial-Interglacial variations in atmospheric pCO_2 involved an increase in the mean-ocean alkalinity during Glacial periods. Increasing alkalinity will cause a decrease in atmospheric pCO_2. Addition to the ocean of alkalinity on Glacial-Interglacial timescales is primarily through continental weathering of carbonate rocks, and the dissolution of shallow and deep-ocean carbonates. Removal of alkalinity from the ocean on these timescales is achieved predominantly through the growth of coral reefs, and through burial of carbonate-shelled organisms in deep-sea sediments. (On Glacial-Interglacial timescales, it is possible that the calcium carbonate reservoir plays and important role in the input *and* removal of alkalinity.) Because the rate of growth and destruction of shallow coral-reefs must vary as sea-level changes between its Interglacial high-stand and the LGM low-stand (some 140m lower), early hypotheses for Glacial-Interglacial variations in atmospheric pCO_2 looked to changes in mean-ocean alkalinity through changes in coral-reef abundance (Berger, 1982; Opdyke and Walker, 1992; Milliman, 1993).

Glacial periods might be expected to correlate with a decrease in coral-reef growth. This would increase mean-ocean alkalinity and ΣCO_2 in the ratio 2:1, and would lead to a decrease in atmospheric pCO_2. An increase in mean-ocean alkalinity would cause an increase in deep ocean CO_3^{2-} which would cause deepening of the calcite lysocline (and hence higher $CaCO_3$ preservation in the deep ocean). Sigman and Boyle (2000) estimate that a 1km average deepening of the lysocline would account for roughly a 25ppmv decrease in atmospheric pCO_2 .

There are two main reasons for the coral-reef hypothesis having been widely rejected. First, this mechanism must be closely correlated with changing sea-level, and clearly much of the sea-level change came after a significant portion of the atmospheric pCO_2 increase coming out of the last glaciation (see section 4.3 and Broecker and Henderson (1998)). Second, a change in mean-ocean alkalinity would trigger a change in the depth of the calcite lyso-

cline, and lysocline depth changes large enough to account for the Glacial-Interglacial atmospheric pCO_2 shift have not been observed. Although it is fairly difficult to assess Glacial-Interglacial changes in the mean calcite lysocline depth from the sedimentary record, in general, there appears to be a consensus that there was slightly higher $CaCO_3$ preservation during the Glacial than at the present day in the Pacific and North Atlantic (Catubig et al., 1998; Farrell and Prell, 1989; Farrell, 1991), and that the calcite lysocline was probably only slightly (order 500m) deeper than during Interglacials (Farrell and Prell, 1989; Berger, 1982).

With a closed-system model, we are not able to simulate how the lysocline will change in response to an alkalinity perturbation. However, we are able to explore how atmospheric pCO_2 in the model will respond to a change in mean-ocean alkalinity. If, starting with the Intermediate-stage (222ppmv) solution, alkalinity is increased in the model by 40μeq/kg, and ΣCO_2 by 20μmol/kg, the response is a decrease in atmospheric pCO_2 from 222ppmv to 210ppmv. This magnitude of change would probably trigger a decrease of order 500m in lysocline depth, which is within the error-bars of observational estimates.

5.4.4 Combined alkalinity and nutrient changes

In order to reconcile our proposed mechanisms with existing observational evidence, it is necessary to invoke a combination of small increase in mean-ocean alkalinity (sufficiently small that the average lysocline depth should be depressed only by a few hundred meters), and a small increase in mean-ocean phosphate (sufficiently small that the thickness of carbonate-rich sediments recorded on existing shallow shelves can account for the change).

Starting with the Intermediate-stage solution (see Table 9), the initial condition for alkalinity was increased by 40μeq/kg and the initial condition for ΣCO_2 by 20μmol/kg. In addition, the initial condition for PO_4 was modified such that there was an increase in mean-ocean phosphate of 0.12μmol/kg (this is the change expected by attributing roughly a third of the observed benthic $\delta^{13}C$ shift to storage in shelf sediments). The solution obtained by making these changes is shown in Table 10. Together, the proposed alkalinity change and whole-ocean nutrient change can account for the remaining depletion of atmospheric pCO_2 from 220ppmv down to LGM levels (c. 196ppmv). In this "Glacial" solution (Table 10), the southern surface-ocean phosphate concentration is close to 1.6μmol/kg, slightly higher than Interglacial levels, which is in agreement with the Cd/Ca data (Elderfield and Rickaby, 2000). Nutrient levels are relatively high in the northern box, and at near-zero levels in the non-polar box. The deep oxygen concentration in this solution is around 60μmol/kg, some 20μmol/kg lower than in the Interglacial solution.

Table 10: *Solution for 'Glacial'. Caption as for Table 8.*

Tracer	A	S	E	N	I	D	B
T	-	-1.72	15.97	1.21	0.21	2.15	0.51
S	-	34.44	35.08	34.83	34.59	34.73	34.61
PO_4	-	1.61	0.07	0.45	2.22	2.34	2.73
ΣCO_2	-	2133.76	1945.48	2036.82	2260.53	2309.41	2349.02
pCO_2	201.46	214.58	203.19	162.18	-	-	-
ALK	-	2322.73	2303.08	2302.74	2354.67	2368.42	2375.72
O_2	-	340.82	253.46	327.74	159.33	58.82	59.08

Benthic $\delta^{13}C$ reached maximum negative values during the Glacial (Duplessy et al., 1988; Curry et al., 1988). By this stage, sea level had fallen sufficiently that large areas of shelf would have been exposed, and any organic material on them could slowly have been eroded into the sea. Our model results indicate that the hypothesized late Glacial increase in mean-ocean phosphate might account for between 6ppmv (volumetric-based change) and 10ppmv of the Glacial atmospheric pCO_2 drawdown. For the remainder of the drawdown we invoke a small change in mean-ocean alkalinity; a likely consequence of increased input of $CaCO_3$ to the ocean via erosion of carbonate-rich rocks on land and coral reefs.

Without the combined action of increase mean-ocean alkalinity and phosphate, it is difficult to explain the last part of the Glacial atmospheric pCO_2 drawdown without violating proxy evidence. Increases in both alkalinity and nutrients are intimately tied to changing sea level. Because detailed sea-level records exist coming out of the Glacial into the Holocene, the feasibility of combined small changes in mean-ocean alkalinity and nutrients can be tested with respect to timing constraints from ice-core records in the transition out of the Glacial.

5.5 Transitioning out of the Glacial Period

It has been observed based on a comparison of the GISP II record of $\delta^{18}O_{atm}$ and the Barbados sea-level curve (Fairbanks, 1989) that $\delta^{18}O_{atm}$ lags changes in sea-level (ice volume) on roughly a 2kyr timescale (Broecker and Henderson, 1998) . These authors make a strong case based on results of $\delta^{18}O_{atm}$

Table 11: *Solution for partial transition out of peak Glacial conditions (235 ppmv). Caption as for Table 8.*

Tracer	A	S	E	N	I	D	B
T	-	0.08	17.96	1.29	1.13	2.76	1.31
S	-	34.49	35.04	34.84	34.59	34.74	34.60
PO_4	-	1.88	0.10	0.43	2.29	2.35	2.68
ΣCO_2	-	2160.99	1957.51	2052.03	2256.46	2311.90	2325.69
pCO_2	234.56	261.88	235.37	176.57	-	-	-
ALK	-	2336.12	2302.32	2302.66	2357.44	2368.85	2373.45
O_2	-	329.93	243.21	327.09	192.79	77.12	113.89

, atmospheric pCO_2, and other proxies from the Vostok ice-core, that the melting of the Northern Hemisphere ice-sheets must have started only after the rise of CO_2 in the atmosphere was well underway. This can be seen from Figure 5, which shows the $\delta^{18}O_{atm}$, atmospheric pCO_2, and dust records from Vostok over the last two terminations.
If the Glacial solution of the model is modified as follows:
1. Southern high latitude mixing is increased back to Interglacial values;
2. The southern box restoring temperature boundary condition is increased from -1.8°C to 0°C (the Interglacial value), and the non-polar restoring temperature boundary condition is increased to 18°C (halfway between the Glacial and Interglacial values), the solution in Table 11 is obtained. Note that there has, as yet, been no increase in the Northern Hemisphere restoring temperature boundary condition. Because this solution does not require any change in Northern Hemisphere temperature or circulation patterns, there are no timing constraints that have been violated.

5.6 Completing the Transition into Full Interglacial Conditions

What remains now is to explain the remainder of the transition back into full Interglacial conditions; the 235-280ppmv part of the record. Close inspection of the Vostok ice-core record shows, during de-glaciations, that the time

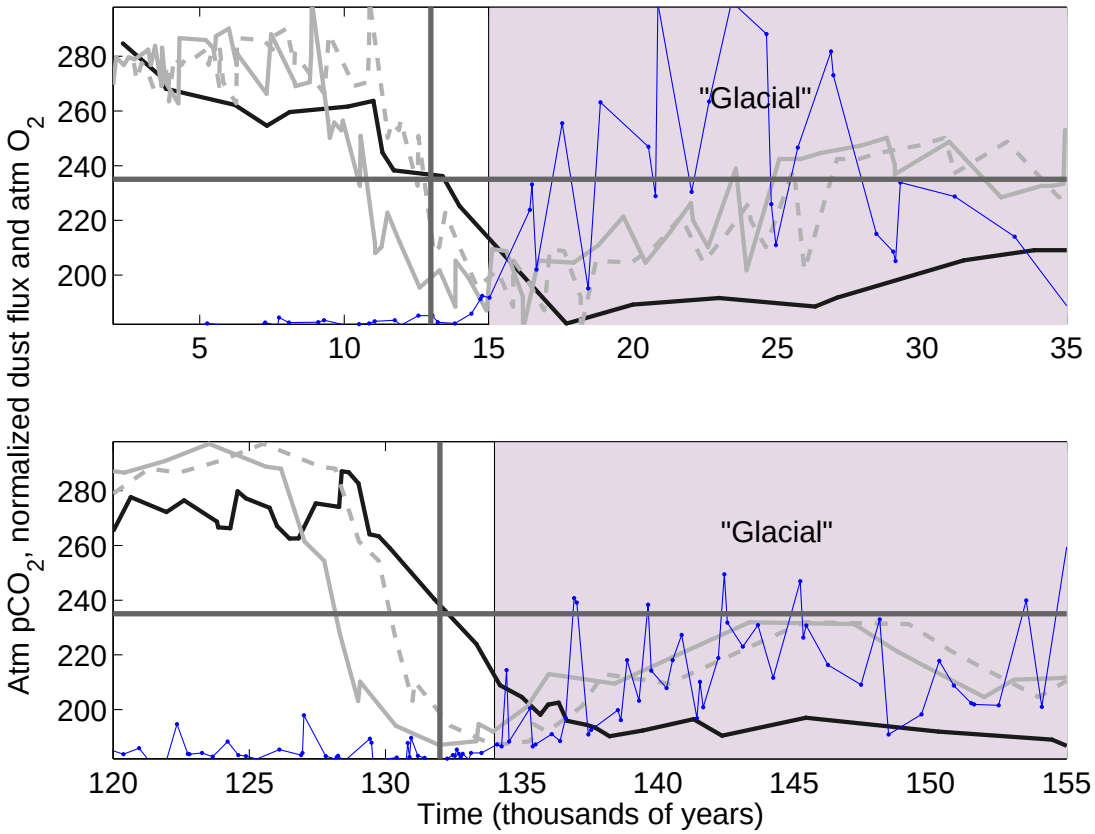

Figure 5: Records of normalized dust (blue), normalized inverted atmospheric δ^{18}O (grey), and pCO_2 (black) from the Vostok ice core over the last two terminations. The dashed line is the atmospheric δ^{18}O curve offset back in time by 2,000 years (so it can be thought of as approximating sea-level). The 235 ppmv ("transitional") atmospheric pCO_2 solution is shown for reference.

at which atmospheric pCO_2 reached intermediate levels (roughly 235ppmv) corresponds to the beginning of the steep rise in atmospheric $\delta^{18}O$ (measured in the air-bubbles in ice; Figure 5). A decrease (increase on the scaled, inverted $\delta^{18}O$ shown in Figure 5) in $\delta^{18}O$ indicates a retreat of ice-sheets over land, or an increase in sea level.

Estimated sea-level curves for the last deglaciation (Fairbanks, 1989; Hanebuth et al., 2000) suggest that the bulk of sea-level rise occurred between 20-10 kyrs B.P. This is consistent with the shifted $\delta^{18}O_{atm}$ record in the Vostok ice-core (Figure 5). Let us therefore accept the Bender et al. (1994) estimate that sea-level starts to rise about 2 kyr before atmospheric $\delta^{18}O$. The dashed grey line in Figure 5 shows $\delta^{18}O_{atm}$ offset by 2 kyrs; the horizontal line shows the transitional 235ppmv solution. It is clear that for both the last two terminations, the point at which atmospheric pCO_2 reached the 235ppmv during the deglaciation corresponds fairly closely to the beginning of the steep rise in shifted $\delta^{18}O_{atm}$, which is here taken as a proxy for sea-level (or Northern Hemisphere ice-sheet melting). For Termination 1, sea-level is about half-way to interglacial levels by the time atmospheric pCO_2 reaches 235ppmv. For Termination 2, however, sea-level is just starting to rise when atmospheric pCO_2 is at the 235ppmv level. Because there will be some timelag between the time at which sea-level starts to rise, and the flooding of the continental shelves, some fraction of total sea-level rise must be accomplished before there is significant deposition of organic-rich shelf sediments.

The entire atmospheric pCO_2 rise (from the Glacial maximum to peak Interglacial) takes order 8kyrs; the mechanism put forth here requires that the first part of the rise (from roughly 200ppmv to 235ppmv) was achieved through gradual Southern Hemisphere and low-latitude warming, melting of southern sea-ice, and subsequent increase in mixing in the Southern Hemisphere. The latter part of the CO_2 rise requires a different explanation; in order to be consistent with our previous hypothesis, we require a sea-level related mechanism. As sea level rose, it would become possible to bury phosphate in organic-rich sediment on the continental shelves, and hence lower the mean ocean phosphate value back to Interglacial levels. Furthermore, growth of coral reefs in shallow seas would alter mean ocean $CaCO_3$, causing a slight lowering of both ΣCO_2 and alkalinity. It must be borne in mind that, for the timing reasons outlined in the previous paragraph, this explanation works better for Termination 1 than for Termination 2.

Changing the temperature restoring boundary condition alone (leaving the high Glacial phosphate levels) back up to its Interglacial values everywhere results in an increase in atmospheric pCO_2 up to 247ppmv; restoring northern hemisphere high-latitude northern mixing back up to Interglacial levels brings the solution to 253ppmv; and finally, and decreasing mean ocean

salinity, phosphate, alkalinity and ΣCO_2 back to those in the Interglacial solution, brings us back to the Interglacial solution presented in Table 8.

6 Discussion and Conclusions

By considering a generalized Glacial-Interglacial cycle to consist of three distinct stages; an "Interglacial", "Intermediate" and "Glacial", we have shown how a distinct sequence of events might account for the observed change in atmospheric pCO_2 between Interglacial and Glacial periods. The initial pCO_2 drawdown, from Interglacial to Intermediate conditions, involves physical changes in the ocean (mixing, tempearture/salinity). The transition from the Intermediate to the Glacial invokes a small increase in mean-ocean nutrient levels and mean-ocean alkalinity. Physical changes in the Southern Ocean (mixing, temperature) are invoked in order to explain the first part of the transition out of peak glacial conditions; the remaining increase in atmospheric pCO_2 (back up to Interglacial levels) is accounted for through a combination of changing ocean chemistry, and changes in the salinity, temperature, and mixing in the northern hemisphere oceans.

The proposed scenario is consistent with most existing evidence on paleonutrient levels and changes in export production over a Glacial-Interglacial cycle. Furthermore, it is consistent with evidence for a whole-ocean shift in $\delta^{13}C$ towards significantly more negative values in the Late Glacial. The proposed sequence of events is also consistent with ice-core-based timing constraints, as summarized by Broecker and Henderson (1998). A short-coming of this study is that we have used a highly simplified "closed-system" model which does not include carbonate dynamics; future work should consider impact of the proposed changes on changes in lysocline depth, and timescales of adjustment, which could be tested in an "open system" model.

The box model we have used here incorporates a dynamic flow-field and a Michaelis-Menten type feedback on export production, and exhibits sensitivities which are somewhat different to models which do not include these effects (Lane et al., 2005). Other distinguishing features of this model are a more realistic export flux than most box models, and parameter values in fair agreement with observations. The model is able to produce both Glacial and Interglacial pCO_2 levels. The model yields tracer distributions in good agreement with observational and proxy evidence. Moreover, as evidenced by the sensitivity analysis discussed in Lane et al. (2005), the model derivatives also appear to be reasonable.

Although we utilized a time-dependent model, we have presented only the steady-state solutions. In order to begin the gradual decline from peak

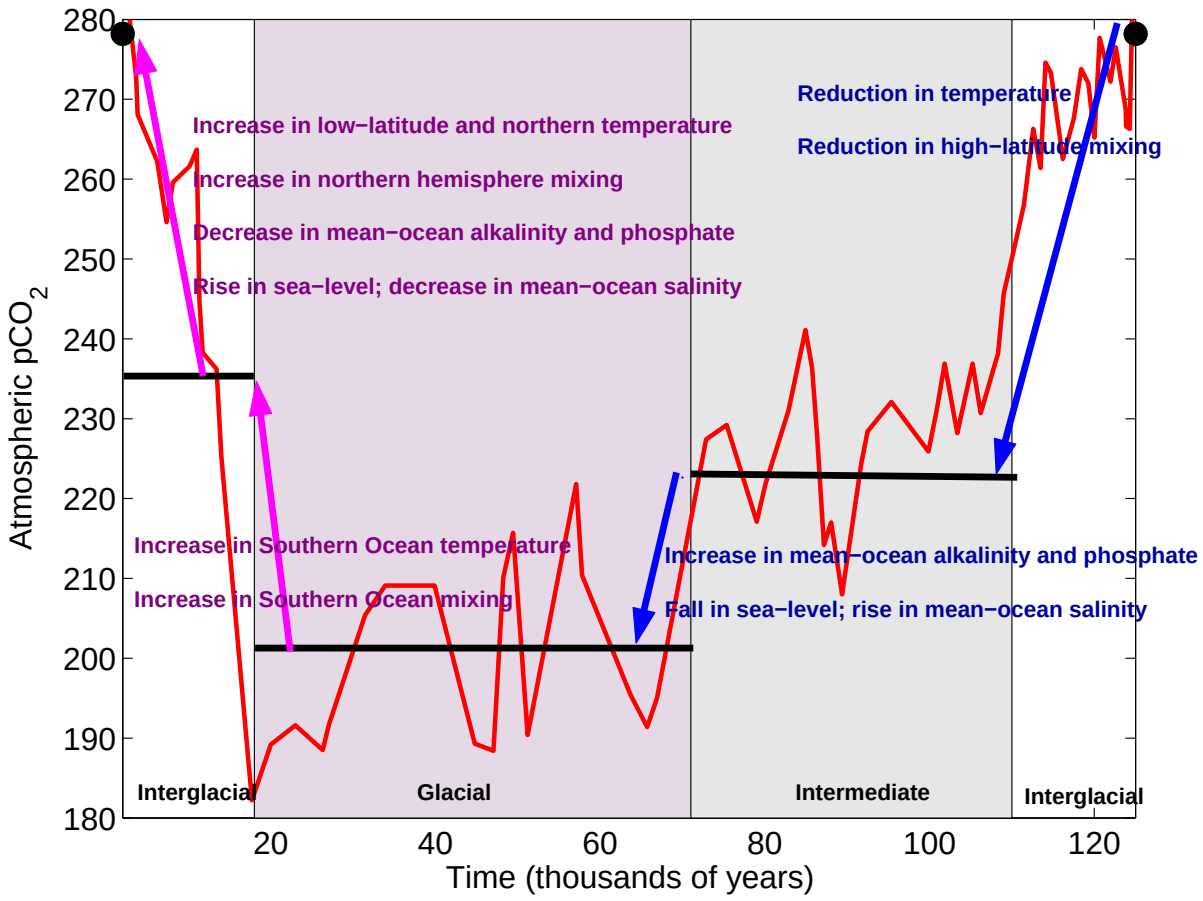

Figure 6: Summary figure showing atmospheric pCO_2 over last Glacial-Interglacial cycle (red), model solutions presented in this study (black horizontal lines), and mechanisms used to explain each part of the observed atmospheric pCO_2 variation (text). The temperature changes in the ocean were achieved in practise by changing the box model restoring boundary conditions as shown in Table 4.

Interglacial to colder, Intermediate-stage conditions, some manner of external forcing would be required. The question of what such a forcing may have been, and why it triggered a 100-kyr cycle (rather than, for example, a 23-Kyr cycle, which would be in line with maxima in insolation change) lies beyond the scope of the present study.

In a most general sense, we envision some external trigger (such as insolation reduction) could feed back to reduce sea-surface temperatures. We speculate that this may feed back to lessen the lateral ocean density gradient and slow the thermohaline circulation, further decreasing sea-surface temperatures. Such a positive feedback between sea-surface temperature and the rate of the overturning circulation could cause an increase in the extent of sea ice, which would slowly reduce atmospheric pCO_2. A gradual increase of sea ice would promote higher stratification in the Southern Ocean water column. As sea-level fell, shelf-areas would gradually become exposed to the atmosphere, and the slow process of erosion could transport the exposed organic-rich shelf sediments and erode carbonate-rich rocks back into the ocean, hence increasing mean-ocean phosphate, ΣCO_2 and alkalinity, and allowing a further draw-down of atmospheric pCO_2 .

In order to make the transition back from full Glacial conditions to the Interglacial state, we also invoke a two-step process. Again, there must be some initial trigger, which may have been a small increase in Southern Hemisphere solar insolation. It is envisioned that this would feedback to increase high-latitude sea-surface temperatures, increase the lateral density gradient in the ocean, increase the rate of the meridional overturning, reduce sea-ice, and to subsequently increase mixing and air-sea gas exchange in the Southern Ocean. Continued warming could (on a timescale of a few thousands of years) lead to melting of the Northern Hemisphere ice sheets and an increase in global sea-level. Flooding of shallow shelf-areas would allow deposition of organic-rich material and growth of coral reefs, causing a slight lowering of mean ocean phosphate, ΣCO_2 and alkalinity.

If growth of sea-ice is responsible for increasing stratification of the high-latitude ocean, it might also be expected that there would be a corresponding decrease in the rate of air-sea gas exchange in the polar oceans. Lowered air-sea gas exchange over the Glacial Southern Ocean has been suggested by Francois et al. (1997) and Stephens and Keeling (2000), among others. We find that if the Southern Ocean air-sea gas exchange term f_{as} is reduced by 20% on top of a modest reduction in high-latitude mixing (30% reduction in the northern box; 40% reduction in the southern box), the atmospheric pCO_2 drops from 222.6ppmv to 222ppmv. In the model presented in this paper, the effect of reducing air-sea gas exchange on atmospheric pCO_2 is so small as to be negligible. This is borne out by the Linearized Sensitivity Analysis performed in a separate paper (Lane et al., 2005). The reduced-

gas-exchange solution does not involve any further change in high latitude nutrient concentrations over the 'Intermediate' stage solution (Table 9); the very slight lowering of atmospheric pCO_2 is achieved through modification of ΣCO_2 and pCO_2 of the surface waters. Reducing southern air-sea exchange results in build-up of ΣCO_2 in the surface southern box (reduced escape for the high-ΣCO_2 deep waters mixing to the surface). This feeds back to slightly reduce the pCO_2 of the atmosphere, which will in turn act to slightly reduce the ΣCO_2 concentration of the non-polar and northern boxes by reducing the air-sea gradient in pCO_2.

In previous studies it has been found that by invoking a single mechanism (e.g. changing mixing, sea-ice-cover, or nutrient utilization, etc), it is very difficult to account for the observed Glacial-Interglacial atmospheric pCO_2 variations. We are in accord with this view, and have therefore sought to explore whether a sequence of events can be found which does not violate the growing body of proxy-evidence for variables such as nutrient levels, export production, etc. Modest changes in physical properties of the ocean (mixing, circulation, temperature) appear sufficient to account for about 55ppmv of the atmospheric pCO_2 drawdown. However, in order to account for the full atmospheric pCO_2 change, we are forced to invoke sea-level related mechanisms. By allowing relatively small changes in mean-ocean alkalinity, ΣCO_2 and phosphate, we show that the remaining 20ppmv of the atmospheric pCO_2 drawdown can be accounted for, and further, that this mechanism does not violate the ice-core-based timing constraints, nor evidence of mean-ocean changes in lysocline depth. Without some storage of organic-rich material on shallow shelves we find are not able to account for the full atmospheric pCO_2 drawdown unless a larger alkalinity change is called upon, and this would require a change in lysocline depth greater than is observed.

Support for the sequence of events proposed here would come from a robust record of the timing of changes in nutrient chemistry of the high-latitude oceans. With the existing data-base of proxy evidence for changes between the Glacial and present-day ocean, the sequence of events we outline in this paper remains just one of many possible scenarios which may explain the observed changes in atmospheric pCO_2 , albeit one that does not violate most existing paleoceanographic evidence. It should be noted that we do *not* require enhanced dust-flux to the surface ocean to play a leading role in the proposed scenario. It appears that the role of the ocean in Glacial-Interglacial atmospheric pCO_2 variations is fairly complex, involving a number of tightly coupled changes. The remarkable similarity of the atmospheric pCO_2 record of each 100-kyr Glacial-Interglacial cycle over the past 430kyrs, as is evident from ice-core records, indicates that whatever these changes in the ocean were, they must have been highly reproducible on timescales of hundreds of thousands of years. Better quantification of possible Glacial-Interglacial

changes in ocean chemistry remains an important challenge for the future.

Acknowledgments:
Thanks to Wally Broecker, who made useful comments on an early version of the manuscript. We are very appreciative of the highly detailed and insightful review by Gideon Henderson, which served to greatly improve the manuscript. Thanks also to one anonymous reviewer for valuable comments.

References

J. F. Adkins, K. McIntyre, and D. P. Schrag. The salinity, temperature, and δ^{18}O of the glacial deep ocean. *Science*, 298:1769–1773, 2002.

L. Anderson and J. Sarmiento. Redfield ratios of remineralization determined by data analysis. *Global Biogeochemical Cycles*, 8:65–80, 1994.

D. Archer and E. Maier-Reimer. Effect of deep-sea sedimentary calcite preservation on atmospheric CO_2 concentration. *Nature*, 367:260–263, 1994.

D. Archer, P. Martin, V. Brovkin, G.-K. Plattner, and C. Ashendel. Model sensitivity in the effect of Antarctic sea ice and stratification on atmospheric pCO_2. *Paleoceanography*, 18 (1):1012, 2003.

D. E. Archer, G. Eschel, A. Winguth, W. Broecker, R. Pierrehumbert, M. Tobis, and R. Jacob. Atmospheric pCO_2 sensitivity to the biological pump in the ocean. *Global Biogeochemical Cycles*, 14 4:1219–1230, 2000.

L. Augustin, C. Barbante, and P. Barnes et al. Eight glacial cycles from an Antarctic ice core. *Nature*, 429:623–628, 2004.

R. B. Bacastow. Vostok ice core provides 160,000 year record of atmospheric CO_2. *Nature*, 329:429–436, 1987.

R. B. Bacastow. The effect of temperature change of the warm surface waters of the oceans on atmospheric CO_2. *Global Biogeochemical Cycles*, 10 (2): 319–334, 1996.

J. Barnola, D. Raynaud, Y. Korotkevich, and C. Lorius. Sea-surface temperature from coral skeletal strontium calcium ratios. *Science*, 257 (5070): 644–647, 1992.

J. W. Beck, R. L. Edwards, E. Ito, F. W. Taylor, J. Recy, F. Rougerie, P. Joannot, and C. Henin. Sea-surface temperature from coral skeletal strontium calcium ratios. *Science*, 257 (5070):644–647, 1992.

M. Bender, T. Sowers, M. Dickson, J. Orchardo, P. Grootes, P. Mayewski, and D. Meese. Dole effect and its variation dyring the last 130,000 years as measured in the vostok ice core. *Global Biogeochemical Cycles*, 8:363–376, 1994.

W. H. Berger. Increase of carbon dioxide in the atmosphere during deglaciation: The coral reef hypothesis. *Naturwissenschaften*, 69:87–88, 1982.

E. A. Boyle. Cadmium and δ^{13}C paleochemical ocean distributions during the stage 2 glacial maximum. *Annual Reviews of Earth and Planetary Sciences*, 20:245–287, 1992.

E. A. Boyle and L. D. Keigwin. Deep circulation of the North Atlantic over the last 200,000 years: Geochemical evidence. *Science*, 218:784–787, 1982.

W. Broecker. *The Glacial world according the Wally.* Eldigio Press, 1995.

W. Broecker, J. Lynch-Stieglitz, D. Archer, M. Hoffman, E. Maier-Reimer, O. Marchal, T. Stocker, and N. Gruber. How strong is the Harvardton-Bear constraint? *Global Biogeochemical Cycles*, 13 4:817–820, 1999.

W. Broecker and T.-H. Peng. *Tracers in the Sea.* Palisades, N.Y. : Lamont-Doherty Geological Observatory, Columbia University, 1982.

W. S. Broecker. Ocean chemistry during Glacial time. *Geochimica et Cosmochimica Acta*, 46:1689–1705, 1982.

W. S. Broecker and G. Henderson. The sequence of events surrounding termination II and their implications for the cause of glacial-interglacial CO_2 changes. *Paleoceanography*, 4:352–364, 1998.

M. Brzezinski, J. Sarmiento, K. Matsumoto, C. Pride, D. Sigman, N. Gruber, G. Rau, and K. Coala. A switch from Si(OH)4 to NO3 depletion in the glacial Southern Ocean. *Geophysical Research Letters*, 29 (12):5.1 – 5.4, 2002.

N. Catubig, D. Archer, R. Francois, P. deMenocal, W. Howard, and E-F. Yu. Global deep-sea burial rate of calcium carbonate during the Last Glacial Maximum. *Paleoceanogaphy*, 13 (3):298–310, 1998.

CLIMAP. "http://ingrid.ldeo.columbia.edu/sources/.climap/", 2001.

M. E. Conkright, S. Levitus, and T. P. Boyer. *World Ocean Atlas. Volumes 1-4.* NOAA Atlas NESDIS 1. U.S. Department of Commerce, Washington, D.C., 1994.

W. Curry, J. C. Duplessy, L. Labeyrie, and N. Shackleton. Changes in the distribution of δ^{13}C of deep water total CO_2 between the last glaciation and the holocene. *Paleoceanography*, 3 (3):317–341, 1988.

C. DeLaRocha, M. Brezinski, M. DeNiro, and A. Shemesh. *Nature*, 395:680, 1998.

J. C. Duplessy, N. Shackleton, R. Fairbanks, L. Labeyrie, D. Oppo, and N. Kallel. Deepwater source variations dyring the last climatic cycle and their impact on the global deepwater circulation. *Paleoceanography*, 3 (3): 343–360, 1988.

H. Elderfield and R. E. M. Rickaby. Oceanic Cd/P ratio and nutrient utilisation in the glacial southern ocean. *Nature*, 405:305–310, 2000.

R. G. Fairbanks. A 17,000 year glacio-eustatic sea level record - influence of glacial melting rates on the Younger Dryas event and deep ocean circulation. *Nature*, 342:637–642, 1989.

P. Falkowski, R. Barber, and V. Smetacek. Biogeochemical controls and feedbacks on ocean primary production. *Science*, 281:200–206, 1998.

J. Farrell. Late neogene paleoceanography of the central equatorial Pacific: evidence from carbonate preservation and stable isotopes. *PhD thesis, Brown Univ. Providence, R.I.*, page 508pp, 1991.

J. Farrell and W. Prell. Climate change and CaCO3 preservation: and 800,000 year bathymetric reconstruction from the central equatorial Pacific Ocean. *Paleoceanography*, 4:447–466, 1989.

R. Francois, M. A. Altabet, E.-F. Yu, D. M. Sigman, M. P. Bacon, M. Frank, G. Bohrman, G. Bareille, and L. Labeyrie. Contribution of Southern Ocean surface-water stratification to low atmospheric CO_2 concentrations during the last glacial period. *Nature*, 389:929–935, 1997.

H. Gildor and E. Tziperman. Physical mechanisms behind biogeochemical glacial-interglacial CO_2 variations. *Geophysical Research Letters*, 27:3077–3080, 2001.

S. J. Goldstein, D. W. Lea, S. Chakraborty, M. Kashgarian, and M. T. Murrell. Uranium-series and radiocarbon geochronology of deep-sea corals: implications for southern ocean ventilation rates and the oceanic carbon cycle. *Earth and Planetary Science Letters*, 193 (1-2):167–182, 2001.

T. P. Guilderson, R. G. Fairbanks, and J. L. Rubenstone. Tropical temperature variations since 20,000 years ago: Modulating inter-hemispheric climate change. *Science*, 263:663–665, 1994.

T. Hanebuth, K. Stattegger, and P. Grootes. Rapid flooding of the Sunda Shelf; a late-glacial sea-level record. *Science*, 288:1033–1035, 2000.

C. Heinze, E. Maier-Reimer, and K. Winn. Glacial pCO_2 reduction by the world ocean: Experiments with the Hamburg carbon cycle model. *Paleoceanography*, 6:295–430, 1991.

F. Knox and M. McElroy. Changes in atmospheric CO_2: Influence of marine biota at high latitude. *Journal of Geophysical Research*, 89 D3:4629–4637, 1984.

K. Kohfeld, C. Le Quere, S. Harrison, and R. Anderson. Limited role of marine biology in glacial-interglacial CO_2 cycles. *Science*, in press, 2005.

N. Kumar, R. F. Anderson, R. A. Mortlock, P. N. Froelich, P. Kubik, B. Dittrich-Hannen, and M. Suter. Increased biological productivity and export production in the glacial Southern Ocean. *Nature*, 378:675–680, 1995.

K. Lambeck and J. Chappell. Sea level change through the last glacial cycle. *Science*, 292:679–686, 2001.

E. Lane, S. Peacock, and J. Restrepo. A dynamic-flow box model and high-latitude sensitivity. *submitted to Tellus B*, 2005.

J. Martin. Glacial-interglacial CO_2 change: the iron hypothesis. *Paleoceanography*, 5 1:1–13, 1990.

P. A. Martin, D. W. Lea, Y. Rosenthal, N. J. Shackleton, M. Sarnthein, and T. Papenfuss. Quaternary deep sea temperature histories derived from benthic foraminiferal Mg/Ca. *Earth and Planetary Science Letters*, 198: 193–209, 2002.

K. Matsumoto, J. Sarmiento, and M. Brezezinski. Silicic acid leakage from the Southern Ocean as possible mechanism for explaining glacial atmospheric pCO_2. *Global Biogeochemical Cycles*, 16 (10), 2002.

J. D. Milliman. Production and accumulation of calcium carbonate in the ocean: budget of a nonsteady state. *Global Biogeochemical Cycles*, 7 (4): 927–957, 1993.

B. N. Opdyke and J. Walker. Return of the coral reef hypothesis: basin to shelf partitioning of CaCO3 and its effect on atmospheric pCO2. *Geology*, 20:733–736, 1992.

J. Petit, J. Jouzel, and D. Raynaud et al. Climate and atmospheric history of the past 420,000 years from the vostok ice core, antarctica. *Nature*, 399: 429–436, 1999.

K. L. Polzin, J. M. Toole, J. R. Ledwell, and R. W. Schmitt. Spatial variability of turbulent mixing in the abyssal ocean. *Science*, 276:93–96, 1997.

A. Ridgwell. *Glacial-interglacial perturbations in the global carbon cycle*. PhD thesis, University of East Anglia, 2001.

R. Robinson, D. Sigman, and B. Brunelle. Revisiting nutrient utilization in the glacial Antarctic: Evidence from a new method for diatom-bound N isotopic analysis. *Paleoceanography*, 19:DOI:10.1029/2003PA00096, 2004.

R. Robinson, D. Sigman, P. DiFiore, M. Rohde, T. Mashiotta, and D. Lea. Diatom-bound 15N/14N: New support for enhanced nutrient consumption in the ice age subantarctic. *Paleoceanography*, 20: DOI:10.1029/2004PA001114, 2005.

E. J Rohling, M. Fenton, F. J. Jorissen, P. Bertrand, G. Ganssen, and J.P. Caulet. Magnitudes of sea-level lowstands of the past 500,000 years. *Nature*, 394:162–165, 1998.

Y. Rosenthal, M. Dahan, and A. Shemesh. *Paleoceanography*, 15:65, 2000.

R. Rutberg and S. Peacock. High-latitude forcing of interior ocean d13c. *submitted to Paleoceanography*, 2005.

J. L. Sarmiento and J. R. Toggweiler. A new model for the role of the oceans in determining atmospheric pCO_2. *Nature*, 308:621–624, 1984.

A. Schimanski and K. Stattegger. Deca-meter-scale holocene sedimentation on the Vietnamese Shelf. *in:European Union of Geosciences conference abstracts*, EUG 11, J. Conf. Abst. Cambr. Publ., Cambridge:pp. 182, 2001.

W. Schmitz. On the interbasin-scale thermohaline circulation. *Reviews of Geophysics*, 33:151–173, 1995.

M. Schultz and A. Paul. Sensitivity of the ocean-atmosphere carbon cycle to ice-covered and ice-free conditions in the nordic seas during the last glacial maximum. *Paleogeography, Paleoclimatology, Paleoecology*, 207:127–141, 2004.

N. J. Shackleton. Tropical rainforest history and the equatorial pacific carbonate dissolution cycles. *in The Fate of Fossil Fuel CO2 in the Oceans*, eds N. R. Anderson and A. Malahoff:Plenum Press, New York. p. 401–428, 1977.

N. J. Shackleton, J.-C. Duplessy, M. Arnold, P. Maurice, M. A. Hall, and J. Cartlidge. Radiocarbon age of last glacial Pacific deep water. *Nature*, 335:708–710, 1988.

M. Siddall, E. Rohling, A. Almogi-Labin, C. Hemleben, D. Meischner, L. Schmelzer, and D. Smeed. Sea-level fluctuations during the last glacial cycle. *Nature*, 423:853–858, 2003.

U. Siegenthaler and T. Wenk. Rapid atmospheric CO_2 variations and ocean circulation. *Nature*, 308:624–626, 1984.

D. M. Sigman and E. A. Boyle. Glacial/interglacial variations in atmospheric carbon dioxide. *Nature*, 407:859–869, 2000.

D. M. Sigman, D. C. McCorkle, and W. Martin. The calcite lysocline as a constraint on glacial/interglacial low-latitude production changes. *Global Biogeochemical Cycles*, 12 (3):409–427, 1998.

E. L. Sikes, C. R. Samson, T. P. Guilderson, and W. R. Howard. Old radiocarbon ages in the southwest Pacific Ocean during the last glacial period and deglaciation. *Nature*, 405 (6786), 2000.

B. Stephens and R. Keeling. The influence of Antarctic sea ice on glacial-interglacial CO_2 variations. *Nature*, 404:171–174, 2000.

T. Takahashi, R. A. Feely, R. F. Weiss, R. H. Wanninkhof, D. W. Chipman, S. C. Sutherland, and T. T. Takahashi. Global air-sea flux of CO_2: An estimate based on measurements of sea-air pCO_2 difference. *Proceedings of the National Academy of Sciences of the United States of America*, 94 #16:8292–8299, 1999.

J. R. Toggweiler. Variations of atmospheric CO_2 by ventilation of the ocean's deepest water. *Paleoceanography*, 5:571–588, 1999.

J. R. Toggweiler, A. Gnanadesikan, S. Carson, R. Murnane, and J. L. Sarmiento. Representation of the carbon cycle in box models and gcms, part 1, the solubility pump. *Global Biogeochemical Cycles*, 17(1), 2003.

A. Winguth, D. Archer, J.-C. Duplessy, E. Maier-Reimer, and U. Mikolajewicz. Sensitivity of paleonutrient tracer distributions and deep-sea circulation to glacial boundary conditions. *Paleoceanography*, 14:304–323, 1999.

C. Wunsch. Determining paleoceanographic circulations, with emphasis on the Last Glacial Maximum. *Wuaternary Science Reviews*, 22:371–385, 2003.

Y. Yokoyama, K. Lambeck, P. De Deckker, P. Johnston, and L. K. Fifield. Timing of the last glacial maximum from observed sea-level minima. *Nature*, 406:713–716, 2000.

E. Yu, R. Francois, and M. Bacon. Similar rates of modern and last-glacial ocean thermohaline circulation inferred from radiocahemical data. *Nature*, 379:689–694, 1996.

List of Figures

1 Atmospheric pCO_2 (red) and dust (blue) records from the Vostok ice core. Data are those reported in Petit et al. (1999). Both records have been normalized such that the maximum values over the time period 0-430,000 years scale to +1, and the minimum values to zero (in absolute terms, over the period shown in the figure, the minimum value of pCO_2 is 182 ppmv and the maximum 298ppmv). The shaded regions correspond to time-periods discussed in the text, and during which each model solution was obtained. The Interglacial (IG) periods are those of high (roughly 280ppmv) atmospheric pCO_2 and low background dust flux; 'Intermediate' (INT) periods occur between full Interglacial and full Glacial conditions (grey shading); and for the purposes of this study, 'Glacial' is used to refer to the period with coldest temperatures, lowest atmospheric pCO_2, and highest dust-flux. . . . 8

2 Diagram of the six-box model (not to scale). Shown are the atmosphere (A), the southern surface box (S), the non-polar, or equatorial surface box (E), the northern surface box (N), the deep southern or intermediate box (I), the deep box (D) and the bottom box (B). The density driven thermohaline flow is shown as Q_1, Q_2, and Q_3. f_{xy} denotes mixing between boxes x and y and pf is the particulate flux. 16

3 Records of normalized dust (blue), normalized, inverted atmospheric $\delta^{18}O$ (grey) and pCO_2 (black) from the Vostok ice core over the last two Glacials. The shading shows the partitioning into "Intermediate" and "Glacial" periods, as defined in the text. 26

4 Dependence on atmospheric pCO_2 on various mixing terms in the box model. The starting point is 257ppmv, achieved by imposing 'Glacial' temperature boundary conditions and salinity initial condition (see Table 3) on the model. The triangles represent changes to only the term f_{ib}; crosses represent changes to only the term f_{nd}; open circles to only the term f_{si}; squares to both the southern box mixing terms simultaneously; and stars to all three high-latitude mixing terms simultaneously. 28

5 Records of normalized dust (blue), normalized inverted atmospheric $\delta^{18}O$ (grey), and pCO_2 (black) from the Vostok ice core over the last two terminations. The dashed line is the atmospheric $\delta^{18}O$ curve offset back in time by 2,000 years (so it can be thought of as approximating sea-level). The 235 ppmv ("transitional") atmospheric pCO_2 solution is shown for reference. 38

6 Summary figure showing atmospheric pCO_2 over last Glacial-Interglacial cycle (red), model solutions presented in this study (black horizontal lines), and mechanisms used to explain each part of the observed atmospheric pCO_2 variation (text). The temperature changes in the ocean were achieved in practise by changing the box model restoring boundary conditions as shown in Table 4. 41

List of Tables

1 *Definition of time periods used in this study* 5
2 *Estimated mixing coefficients, effective fluxes, areas and length-scales from the Interglacial model solution. Area and length scale were prescribed a priori.* 17
3 *Parameter values used in all model solutions* 18
4 *Parameter values used which differed for the Glacial, Intermediate, and Interglacial solutions.* 19
5 *Flow rates obtained for thermohaline flow obtained from Interglacial, Intermediate, and Glacial solutions.* 19
6 *Export Flux of Carbon out of each surface box obtained from Interglacial, Intermediate and Glacial solutions.* 19
7 *Mean and standard deviations (s.d.) for temperature, salinity and oxygen in the regions of the ocean corresponding to the different model boxes. Values were computed from the Levitus annual average dataset, with the Arctic Ocean excluded from the averaging due to spurious values in this region. Values are given for the southern surface box (S), the non-polar, or equatorial surface box (E), the northern surface box (N), the deep southern or intermediate box (I), the deep box (D) and the bottom box (B).* 21
8 *Solution for Interglacial ocean. Temperature is given in $^\circ C$, salinity in $‰$. The concentrations of PO_4, ΣCO_2 and O_2 are given in $\mu mol/kg$, pCO_2 is given in ppmv and alkalinity is given in $\mu eq/kg$. A, S, E, N, I, D and B correspond to the regions illustrated in Figure 1.* 24
9 *Solution for "Intermediate" stage. Caption as for Table 8.* . 30
10 *Solution for 'Glacial'. Caption as for Table 8.* 36
11 *Solution for partial transition out of peak Glacial conditions (235 ppmv). Caption as for Table 8.* 37